



NAVAL POSTGRADUATE SCHOOL

MONTEREY, CALIFORNIA

THESIS

ANTI-SUBMARINE WARFARE SEARCH MODELS

by

Roey Ben Yoash

September 2016

Thesis Co-Advisors:

Moshe Kress

Michael Atkinson

Second Reader:

Roberto Szechtman

Approved for public release. Distribution is unlimited.

THIS PAGE INTENTIONALLY LEFT BLANK

REPORT DOCUMENTATION PAGE			<i>Form Approved OMB No. 0704-0188</i>	
Public reporting burden for this collection of information is estimated to average 1 hour per response, including the time for reviewing instruction, searching existing data sources, gathering and maintaining the data needed, and completing and reviewing the collection of information. Send comments regarding this burden estimate or any other aspect of this collection of information, including suggestions for reducing this burden, to Washington headquarters Services, Directorate for Information Operations and Reports, 1215 Jefferson Davis Highway, Suite 1204, Arlington, VA 22202-4302, and to the Office of Management and Budget, Paperwork Reduction Project (0704-0188) Washington, DC 20503.				
1. AGENCY USE ONLY (Leave blank)		2. REPORT DATE September 2016		3. REPORT TYPE AND DATES COVERED Master's thesis
4. TITLE AND SUBTITLE ANTI-SUBMARINE WARFARE SEARCH MODELS			5. FUNDING NUMBERS	
6. AUTHOR(S) Roey Ben Yoash				
7. PERFORMING ORGANIZATION NAME(S) AND ADDRESS(ES) Naval Postgraduate School Monterey, CA 93943-5000			8. PERFORMING ORGANIZATION REPORT NUMBER	
9. SPONSORING /MONITORING AGENCY NAME(S) AND ADDRESS(ES) N/A			10. SPONSORING / MONITORING AGENCY REPORT NUMBER	
11. SUPPLEMENTARY NOTES The views expressed in this thesis are those of the author and do not reflect the official policy or position of the Department of Defense or the U.S. Government. IRB Protocol number ____N/A____.				
12a. DISTRIBUTION / AVAILABILITY STATEMENT Approved for public release. Distribution is unlimited.			12b. DISTRIBUTION CODE A	
13. ABSTRACT (maximum 200 words) Stealth and high endurance make submarines ideally suited to a variety of missions, and finding ways to detect, track, and, if necessary, acquire and attack them has long been a topic of research. In this thesis, we study effective ways to operate an MH-60R helicopter in anti-submarine warfare (ASW) missions. Following an initial cue given by an external source indicating the presence of a possible submarine target, a helicopter is sent to detect, follow, acquire, and attack the submarine. To perform its mission, the helicopter can carry various payloads of sensors and torpedoes. The first part of the thesis focuses on a helicopter equipped with dipping sonar and develops a model that optimizes the operation of the helicopter and measures its effectiveness. We analyze the effect of the different input parameters, such as helicopter speed, submarine speed, sensor detection radius, and travel time to the point of detection on the optimal dipping pattern and the probability of mission success, and show that arrival time is the most important parameter. We also address the optimization problem associated with the payload of a helicopter on an ASW mission and determine the best mix of fuel, sensors, and weapons for a helicopter on such a mission.				
14. SUBJECT TERMS Anti-submarine warfare, search and detection			15. NUMBER OF PAGES 85	
			16. PRICE CODE	
17. SECURITY CLASSIFICATION OF REPORT Unclassified	18. SECURITY CLASSIFICATION OF THIS PAGE Unclassified	19. SECURITY CLASSIFICATION OF ABSTRACT Unclassified	20. LIMITATION OF ABSTRACT UU	

THIS PAGE INTENTIONALLY LEFT BLANK

Approved for public release. Distribution is unlimited.

ANTI-SUBMARINE WARFARE SEARCH MODELS

Roey Ben Yoash
Captain, Israel Defense Forces
B.Sc., The Hebrew University of Jerusalem, 2010

Submitted in partial fulfillment of the
requirements for the degree of

MASTER OF SCIENCE IN OPERATIONS RESEARCH

from the

NAVAL POSTGRADUATE SCHOOL
September 2016

Approved by: Moshe Kress
Thesis Co-Advisor

Michael Atkinson
Thesis Co-Advisor

Roberto Szechtman
Second Reader

Patricia Jacobs
Chair, Department of Operations Research

THIS PAGE INTENTIONALLY LEFT BLANK

ABSTRACT

Stealth and high endurance make submarines ideally suited to a variety of missions, and finding ways to detect, track, and, if necessary, acquire and attack them has long been a topic of research. In this thesis, we study effective ways to operate an MH-60R helicopter in anti-submarine warfare (ASW) missions. Following an initial cue given by an external source indicating the presence of a possible submarine target, a helicopter is sent to detect, follow, acquire, and attack the submarine. To perform its mission, the helicopter can carry various payloads of sensors and torpedoes. The first part of the thesis focuses on a helicopter equipped with dipping sonar and develops a model that optimizes the operation of the helicopter and measures its effectiveness. We analyze the effect of the different input parameters, such as helicopter speed, submarine speed, sensor detection radius, and travel time to the point of detection on the optimal dipping pattern and the probability of mission success, and show that arrival time is the most important parameter. We also address the optimization problem associated with the payload of a helicopter on an ASW mission and determine the best mix of fuel, sensors, and weapons for a helicopter on such a mission.

THIS PAGE INTENTIONALLY LEFT BLANK

TABLE OF CONTENTS

I.	INTRODUCTION.....	1
A.	MOTIVATION	1
B.	LITERATURE REVIEW	1
C.	OPERATIONAL SETTING AND OBJECTIVE	2
D.	SCOPE, LIMITATIONS, AND ASSUMPTIONS	3
E.	THESIS OUTLINE.....	3
II.	UNIFORM DIRECTION.....	5
A.	NOTATION AND DEFINITIONS.....	7
B.	MAIN RESULT	10
C.	NUMERICAL RESULTS	11
1.	Helicopter's Speed	11
2.	Arrival Time	14
3.	Time per Dip.....	15
4.	Dipper's Detection Range.....	17
5.	Submarine's Speed.....	21
D.	PROOF OF THE OPTIMAL DIPPING PATTERN	22
E.	TWO SPEEDS MODEL	30
F.	BUOYS.....	32
III.	NON-UNIFORM DIRECTION.....	37
A.	THREE RAYS MODEL	37
1.	Model Description	37
2.	Model Results	42
B.	FIVE RAYS MODEL	46
1.	Model Description	46
2.	Model Results	48
C.	THREE WEDGES MODEL	50
1.	Model Description	50
2.	Model Results	52
IV.	PAYLOAD OPTIMIZATION.....	57
A.	DETECTION MISSION	58
B.	ATTACK MISSION	60

V.	CONCLUSION	63
A.	SUMMARY	63
B.	FOLLOW-ON WORK.....	64
	LIST OF REFERENCES	65
	INITIAL DISTRIBUTION LIST	67

LIST OF FIGURES

Figure 1.	MH-60R Equipped with a Dipper.....	6
Figure 2.	Direction Angle.....	8
Figure 3.	Coverage Angle	8
Figure 4.	Disjoint and Non-Disjoint Dips	9
Figure 5.	Effective Coverage Angle.....	10
Figure 6.	Example of an Optimal Dipping Pattern.....	11
Figure 7.	Spirals when Varying the Helicopter Speed (50, 100, and 200 Knots)	12
Figure 8.	Number of Dips and Time to Complete Coverage vs. Helicopter's Speed.....	13
Figure 9.	Spirals When Varying the Arrival Time (0.5, 1 and 1.5 Hours).....	14
Figure 10.	Number of Dips and Time to Complete Coverage vs. Arrival Time.....	15
Figure 11.	Spirals with Varying Dipping Times (2.5, 5 and 10 Minutes per Dip)	16
Figure 12.	Number of Dips and Time to Complete Coverage vs. Time per Dip	17
Figure 13.	Spirals with Varying Detection Radii (1.5, 3, and 6 NM)	18
Figure 14.	Number of Dips and Time to Complete Coverage vs. Detection Radius	19
Figure 15.	Zoom-in on Time and Dips for Complete Coverage vs. Detection Radius	20
Figure 16.	Spirals with Varying Submarine Speeds (4, 8, and 16 Knots).....	21
Figure 17.	Time and Dips for Complete Coverage vs. Submarine's Speed.....	22
Figure 18.	Calculation of Coverage Angle.....	23
Figure 19.	Optimal Next Dipping Location	24
Figure 20.	Definition of ω	25
Figure 21.	ω as a Function of T	25

Figure 22.	Overlap Calculation	27
Figure 23.	Proof by Contradiction.....	28
Figure 24.	Intermediate Value Theorem	29
Figure 25.	Two Speed Options for Dipping Patterns. Slower First (left) and Faster First (right)	30
Figure 26.	Two Speeds, Detection Time vs. Probability of Target Moving at Faster Speed.....	31
Figure 27.	Comparing Detection Radius and Dipping Time, Showing the Log of Time to Complete Coverage	33
Figure 28.	Buoy Placement	34
Figure 29.	Three Rays Model.....	38
Figure 30.	Flight between Rays.....	40
Figure 31.	Three Rays, $S = 10$, $\theta = 120^\circ$	43
Figure 32.	Three Rays, $\theta = 90^\circ$ Different Values of S	44
Figure 33.	Three rays, $S = 10$, Varying Angle	45
Figure 34.	Five Rays Model.....	46
Figure 35.	Five Rays Model $S = 10$, $\theta = 45^\circ$	48
Figure 36.	Five Rays Model, Ratio =10, Varying Angle	49
Figure 37.	Five Rays Model, $\theta = 30$, S Varied.....	50
Figure 38.	Three Wedges Model.....	51
Figure 39.	Three Wedges Model, $\alpha = \beta = \gamma = 30^\circ$, $S = 10$	52
Figure 40.	Three Wedges Model, $S = 10$, $\beta = 30$, α and γ Varied.....	53
Figure 41.	Three Wedges Model, $S = 10$, $\alpha = \gamma = 30^\circ$ and β Varied.....	54
Figure 42.	Three Wedges Model, $S = 10$, $\alpha = \beta = 30^\circ$ and γ Varied.....	55
Figure 43.	Three Wedges Model, $\alpha = \beta = \gamma = 30^\circ$, S Varied.....	56

Figure 44.	Probability of Detection vs. Number of Buoys, Arrival Time 1 Hour, Speed Ratio 10	58
Figure 45.	Coverage vs. Number of Buoys, Arrival Time Varied	59
Figure 46.	Probability of Mission Success with Different Number of Torpedoes.....	60
Figure 47.	Probability of Success vs. Arrival Time	61
Figure 48.	Probability of Success vs. Arrival Time, Varying P_k	62

THIS PAGE INTENTIONALLY LEFT BLANK

EXECUTIVE SUMMARY

Submarines have been an important part of the military for more than a century. Their stealth, together with their high endurance, allows them to stay undetected for long periods of time and surprise the enemy, anywhere, without notice.

As technology improves, so do the capabilities of submarines. Submarines can perform a wide range of missions, including attacking other submarines, attacking surface vessels, launching cruise and ballistic missiles, and gathering intelligence. This is why enemy submarines are considered very dangerous to friendly forces, and anti-submarine warfare (ASW) is considered an important mission for submarines, surface vessels, fixed wing aircraft, and helicopters.

Since submarines are hard to detect, finding ways to optimize the search for and attack on enemy submarines is very important. The effort to do so started as early as World War II, and was one of the building blocks of operations research and search theory. Several books and papers have been published that formulate various types of search models.

In this thesis, we focus on a submarine hunt mission performed by a helicopter such as an MH-60R SEAHAWK. Such a mission begins with an initial signal from an external source, pointing to the possible location of an enemy submarine in the area. The point of detection is called a *datum*. The helicopter is then sent to the datum to detect, follow, and, if needed, acquire and attack the target submarine.

We first derive an optimal dipping pattern for a helicopter carrying dipping sonar, assuming the submarine's speed is known but its direction is unknown. The Area of Uncertainty (AoU) in this scenario is the circumference of a circle, growing bigger as time passes since the submarine is moving away from the datum. The dipping pattern in this scenario is a spiral, which grows together with the AoU. After every dip, the searching helicopter has to consider a trade-off; on one hand, the tendency is to dip as late as possible to avoid overlap with the previous dip, but on the other hand, it would be better to dip sooner so that the AoU does not grow too large. We prove the optimality of

our pattern and analyze the effect the scenario parameters have on the results, mainly the time and number of dips needed to ensure detection. We show that the arrival time at the datum is the most important parameter. We also show that our pattern is optimal for a helicopter carrying sonobuoys as well and analyze the differences in the operation behavior between carrying sonobuoys and a dipper.

Next, we assume that there is some knowledge about the submarine's direction of movement. We present two models for this scenario: a ray model and a wedge model. In the ray model, the target moves along one of a discrete number of rays, and the searcher needs to choose the order in which to search the rays. During this search, the searcher might skip over rays to get to other rays with higher probabilities of the target moving along those rays. Although this will bring the searcher to the high priority rays faster, this might cause him to fly back and forth, and waste time. We analyze this trade-off and the effect of the scenario parameters. Scenario (c), which involves three wedges, combines our initial continuous model with our ray model into a more realistic non-uniform direction model.

Finally, we address a different aspect of the ASW problem. Helicopters are very limited in the weight and volume they can carry. For an ASW mission, the helicopter needs to carry fuel for endurance, sensors for detection, and torpedoes for attacking. We address two types of missions: a) detection and b) attack. For detection missions, we analyze the optimal payload of sonobuoys and fuel. If the searcher carries too many buoys, then the helicopter might run out of fuel and will have to return without using all of its buoys. If the helicopter carries too much fuel, then it might run out of buoys and return with extra fuel. For attack missions, we need to balance fuel and sonobuoys, which increase the probability of detection, with torpedoes, which increase the probability of kill given a detection. In this type of mission, if the helicopter carries too many torpedoes, the probability of detection decreases, which increases the chances the helicopter will not use the torpedoes. If the helicopter carries too few torpedoes, then it risks detecting the target but being unable to kill it. We analyze the effect the scenario parameters have on the optimal payload, showing that the arrival time to the datum is the most important parameter in determining the optimal payload.

ACKNOWLEDGMENTS

I would like to thank my advisors, Moshe Kress and Michael Atkinson, for their guidance and for their help in turning ideas into a thesis.

I would also like to thank the rest of the Operations Research faculty at the Naval Postgraduate School for giving me the tools to successfully complete this thesis.

THIS PAGE INTENTIONALLY LEFT BLANK

I. INTRODUCTION

A. MOTIVATION

In today's warfare, as in the past, submarines play a very important operational and strategic role. Their stealth, combined with the advent of new technologies such as long-range missiles, opens up a wide range of capabilities for undersea warfare. From intelligence collecting through attacking surface vessels to launching nuclear missiles, submarines can surprise the enemy—anywhere, anytime.

With the growing capabilities of submarines such as quieter engines and longer underwater endurance, it becomes increasingly important to be able to effectively find and attack enemy submarines. Several assets can execute anti-submarine warfare (ASW) missions. These include surface vessels, submarines, fixed wing aircraft, and helicopters, all of which can carry both detection sensors and torpedoes for attacking.

In this thesis, we focus on the ASW helicopter MH-60R SEAHAWK. We examine effective ways to operate MH-60R helicopters in ASW missions. A typical mission for such a helicopter begins with an initial cue by an external source such as a fixed-wing surveillance aircraft, indicating the presence of a suspicious object in the area of interest. The point of detection is called a *datum*. Following such a cue, a helicopter is sent to detect, follow, and, if needed, acquire and attack, the target submarine. To perform its mission, the helicopter can carry various payloads, including sonobuoys and a dipping sonar to detect the target, and torpedoes to attack it.

B. LITERATURE REVIEW

The topic of search and detection has been extensively studied, and various models offer search patterns for different scenarios. From as early as 1946, when Koopman published the analysis done in World War II and laid the foundation for search theory, studies have continued all the way to recent years Stone et al. (2016). Some of the work done includes books dedicated to the topic such as Washburn (2002), Stone (1975), and Haley and Stone (1980), which discuss and develop several search and detection models and provide the reader with operational examples on how to use those models.

These books cover a wide range of generic search and detection models and provide the tools to understand and analyze specific scenarios.

The second type of work done in the field of search and detection involves the analysis of specific operational scenarios, the effect of a specific parameter, or the presentation of a new idea. Such work includes Shephard et al. (1988) which presents to the reader several operational scenarios, and then provides possible models to address those scenarios. More recently, Kuhn (2014) examines active multistatic sonar networks. This kind of work usually focuses more on a very specific scenario and considers a small number of parameters.

Other work also involves estimating the effectiveness of search models. Such work includes Washburn (1978), which provides an algorithm for estimating upper bounds on detection probabilities, and Forrest (1993), which uses models to estimate the effectiveness of detection systems.

C. OPERATIONAL SETTING AND OBJECTIVE

We model a scenario in which a naval task force is equipped with an antisubmarine warfare helicopter whose role is to hunt and kill enemy submarines. The helicopter is dispatched on such a mission upon receipt of information about the location (range and direction) of a submarine target. The source of such information might be a long-range airborne anti-sub unit patrolling continuously within the operational area of the task force (P-3/8 aircraft or a surface ship equipped with a sonar device).

Launching helicopters for ASW missions is expensive both economically—the operations costs are high, combining fuel, manpower, and maintenance—and operationally the helicopter may have other competing missions and performing an ASW mission may mean less time for other missions. Given a datum obtained from some external sensor or other information, is it worthwhile to send a helicopter out to search for the target? The answer to this operational question depends on the probability of finding the target and on tactical constraints applicable at that time. We formulate a model—implemented in a spreadsheet tool—to compute the probability of success so that the tactical go/no-go decision can be made more effectively.

If we decide to send out a helicopter for the ASW mission, we face additional questions regarding the optimal mission parameters. First, what is the helicopter's optimal speed on the way to the datum? A faster velocity will allow the helicopter to arrive at the target more quickly and therefore limit the Area of Uncertainty (AoU), the possible location of the target submarine. However, high speeds increase fuel consumption (quasi-quadratic in relation to speed), and thus may reduce the search time for the target once the helicopter reaches the target area. Secondly, the typical payload of a helicopter in an ASW mission comprises active and passive sonobuoys, dipping sonar, torpedoes, and fuel. The mix of these payload types determines the balance among detection capabilities, lethality, and endurance—the “eyes,” “fist,” and “lungs” of the ASW weapon. This balance certainly depends upon the mission and the tactical parameters of the associated scenario. For example, if we only want to find and localize the submarine, we clearly do not need torpedoes and would want to carry more sensors for better coverage or more fuel for higher endurance. Finally, given the payload, what is an effective way to deploy the sensors. For example, if we only have a dipper sonar, what pattern should we use to maximize the detection probability.

D. SCOPE, LIMITATIONS, AND ASSUMPTIONS

As mentioned previously, the effectiveness of search models depends on the scenario and assumptions made, and one can never perfectly model an operational scenario. Each chapter of this work has a different set of assumptions, all stated at the beginning of the chapter. The common theme to most of our assumptions is that they are optimistic. Operationally, this means that the estimates we show correspond to “best case scenario.”

In this work, we only analyze the models for a single helicopter, and the models might change when two or more helicopters are involved in the mission.

E. THESIS OUTLINE

In Chapters II and III, we present several search scenarios and examine them. We examine how varying the inputs to the problem, such as the speeds of the submarine and helicopter and the distance to the target, affect the expected time to detection and the

probability of detection. These insights can be used to enhance ASW mission planning and help make a more informative go/no-go decision. We also compare using sonobuoys to using a dipper. Chapter IV addresses a slightly different problem. We study the effect of payload composition of the ASW helicopter and optimize fuel, sensor, and missiles in order to maximize the probability of a successful mission.

II. UNIFORM DIRECTION

In this chapter, we consider the following problem. An external surveillance source detects an adversary submarine at a certain datum. This information is passed on to an ASW helicopter (e.g., an MH-60R), which is not yet at the site and therefore has to fly to the datum.

We assume that the submarine is not aware that the helicopter is searching the area looking for it, and therefore the submarine keeps moving at a constant speed known to the searcher and in a constant direction, which is unknown to the searcher. This assumption makes the AoU (i.e., area containing the possible location of the submarine) the circumference of a circle, which is centered around the datum. We first assume a uniform distribution on the direction of travel of the submarine, i.e., the submarine might be moving in any direction with equal likelihood. We relax this assumption in the next chapter.

The search helicopter is equipped with dipping sonar (henceforth referred to as a *dipper*), which is “a sonar transducer that is lowered into the water from a hovering antisubmarine warfare helicopter and recovered after the search is complete.”¹ Figure 1 shows an MH-60R helicopter equipped with a dipper.

¹ *The Free Dictionary by Farlex*, s.v. “Dipping sonar,” retrieved June 7, 2016, <http://encyclopedia2.thefreedictionary.com/dipping+sonar>.



Source: USN photography, photo ID: 030100-N-9999Z-001, retrieved August 8, 2016, https://en.wikipedia.org/wiki/Sikorsky_SH-60_Seahawk

Figure 1. MH-60R Equipped with a Dipper

We assume that the dipper has a two-dimensional cookie-cutter detection function with range R . That is, the detection function is in fact an arbitrarily long (i.e., deep) cylinder with radius R . Thus, we ignore possible evasive actions by the submarine going deeper or shallower.

Our goal is to find for the helicopter the best dipping pattern—a series of points in the sea where the dipper is deployed. We define an optimal dipping pattern to be one that given a finite number of dips maximizes probability of detection or, given an infinite number of dips, minimizes the expected time to detection. For example, if the helicopter can only detect the target when the helicopter is directly over it, the helicopter will have to fly in a spiral form, with radial speed as dictated by the submarine speed, in order to stay above the possible location of the submarine, as explained in Washburn (1980).

A. NOTATION AND DEFINITIONS

In this chapter, we use the following notation and definitions.

Inputs to the problems:

U —submarine's speed.

V —speed of the search helicopter.

R —dipper's detection range.

T —time since initial detection by the external source.

T_A - helicopters arrival time to the datum.

Definitions used to describe a dip:

X_i —the X-axis value of the i-th dip.

Y_i —the Y-axis value of the i-th dip.

T_i —the time of the i-th dip (since initial detection by the external source).

K_i —the distance of the i-th dip from the datum. $K_i^2 = X_i^2 + Y_i^2$ and also because the submarine's speed is constant $K_i = U \times T_i$.

D_i —the detected area when dipping the i-th dip, which is a circle with radius R centered at (X_i, Y_i) , i.e., $\forall (X, Y)$ s.t. $(X - X_i)^2 + (Y - Y_i)^2 \leq R^2$.

C_i —the location circumference. This is the geometric description (circle) of the submarine's possible location at the time of the i-th dip. Since the submarine moves in a known constant speed U and constant unknown direction, this is the circumference of a circle with a radius that equals the distance of the i-th dip from the datum, which we denote K_i , i.e. $\forall (X, Y)$ s.t. $X^2 + Y^2 = K_i^2 = (U \times T_i)^2$.

θ_i —direction angle. The angle, rooted at the datum, between the vertical axis and the ray connecting to a dipping point P_i , as shown in Figure 2.

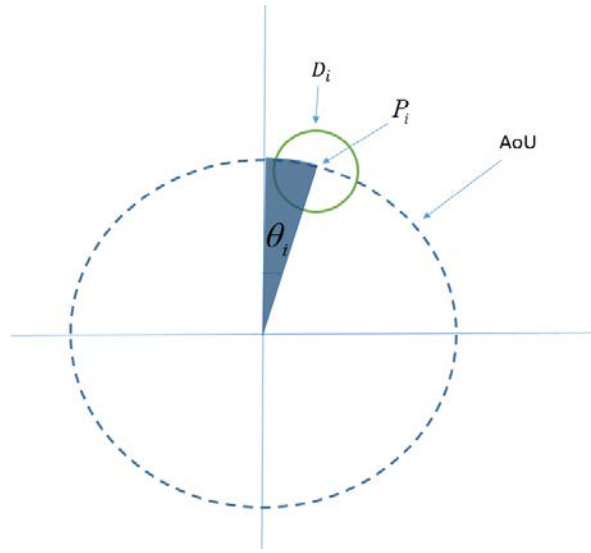


Figure 2. Direction Angle

α_i —coverage angle. An angle rooted at the datum that is determined by the two tangents to the detected area, as shown in Figure 3.

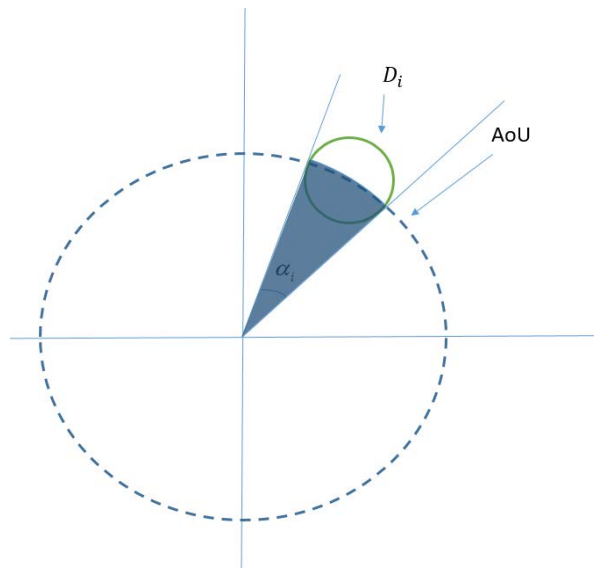


Figure 3. Coverage Angle

We now define terms related to a dipping process:

Dipping pattern—a set of points, P_i , where P_i is the point of the i -th dip. P_i must lay on C_i , so the helicopter can detect the submarine.

$Dist_{i,j}$ —the distance between the i -th and the j -th point of a given dipping pattern, $Dist_{i,j} = \sqrt{(X_i - X_j)^2 + (Y_i - Y_j)^2}$.

Disjoint dips—We call two dips disjoint if no ray from the datum intersects both their corresponding detection areas. In particular, this means that there is no overlap in their respective angular coverage (see Definition 12). Figure 4 illustrates this concept.

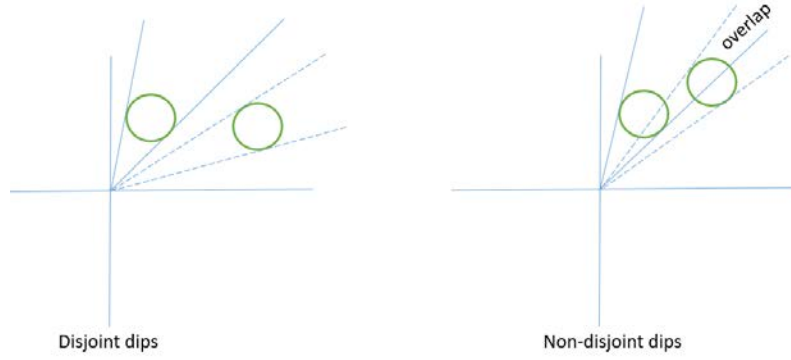


Figure 4. Disjoint and Non-Disjoint Dips

β_i —Effective coverage angle. The angular slice of the AoU covered by a certain dip and not covered by any previous dip. For disjoint dips, the effective coverage angle is the coverage angle α itself. For overlapping dips, the effective coverage of the second dip is smaller than the actual angular coverage because of the overlap, which is already covered by the earlier dip, and therefore does not give us any new information. Figure 5 illustrates this concept.

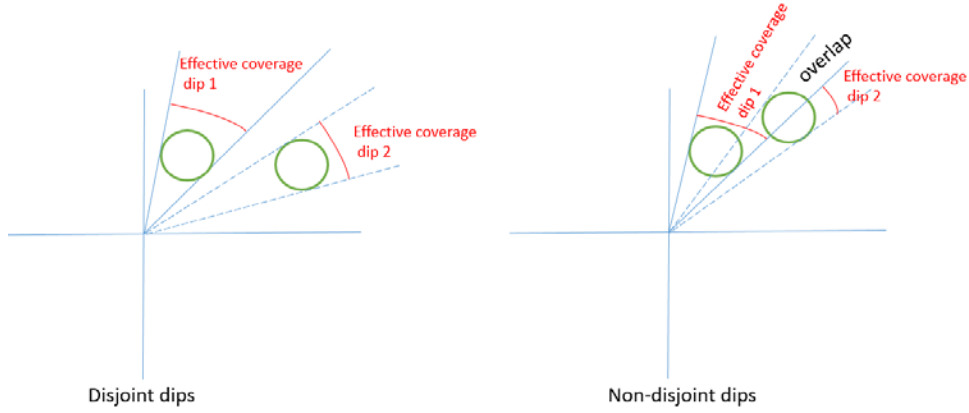
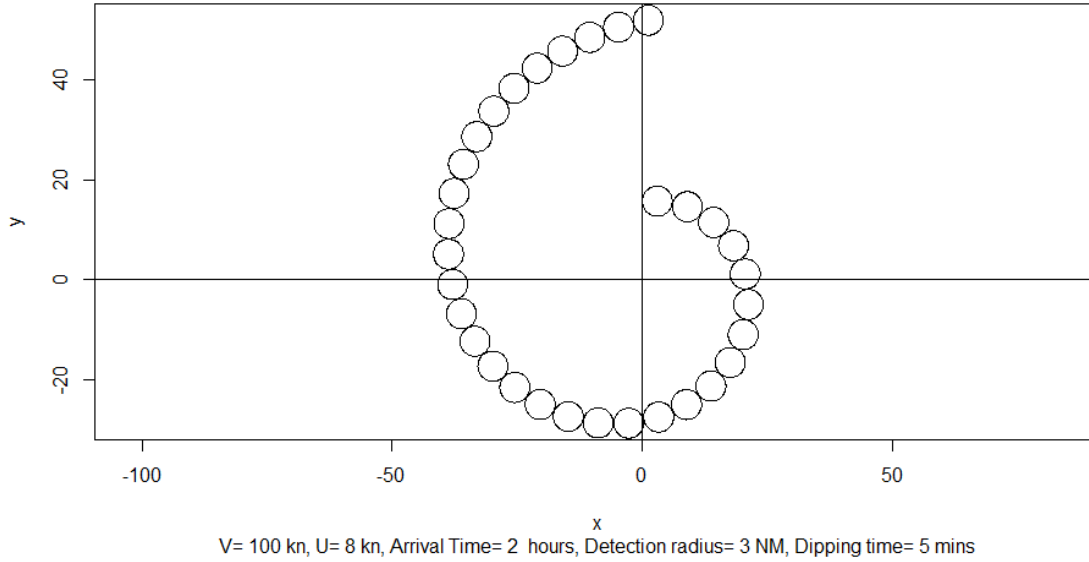


Figure 5. Effective Coverage Angle

B. MAIN RESULT

We are interested in the optimal dipping pattern for the helicopter. There are two competing effects that affect this pattern. The first one is that we want to dip as close as possible to the datum, because then we have bigger coverage angle. This implies that after a dip we would want to dip again as soon as possible. On the other hand, we want to minimize overlap, so each time we dip we get the maximum effectiveness of that dip. That means we do not want to dip too soon after a previous dip because we will have overlap.

We found that the best dipping pattern is the “sweet spot” between those two effects. We dip again as soon as we possibly can without having overlap. This dipping pattern creates a spiral around the datum, as shown in Figure 6.



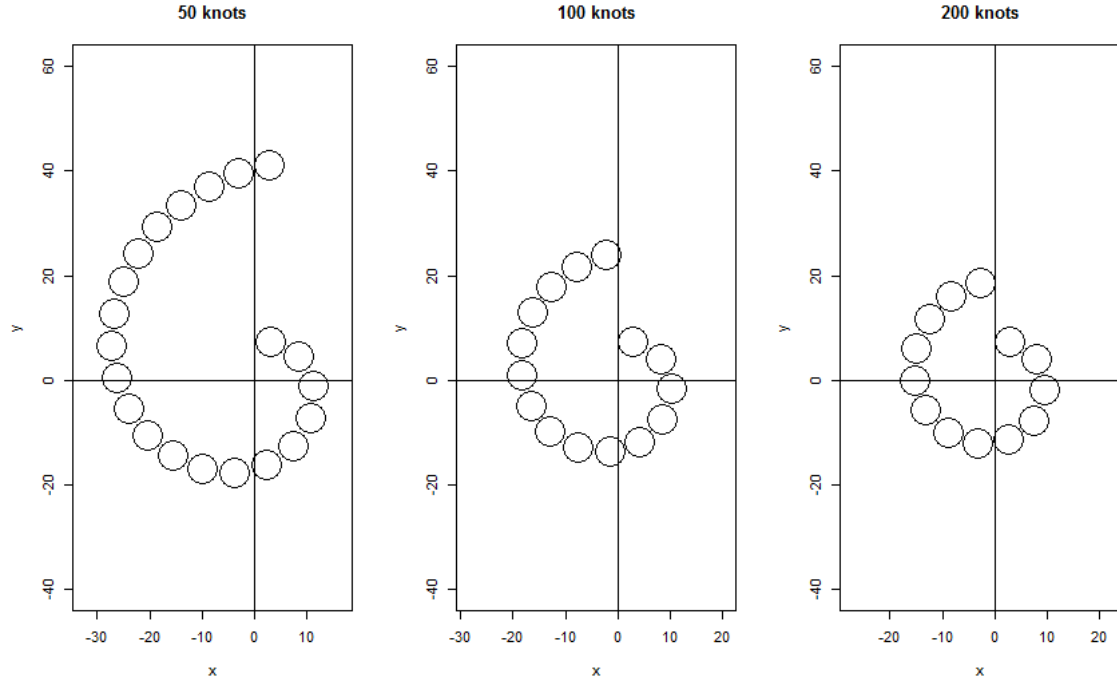


Figure 7. Spirals when Varying the Helicopter Speed (50, 100, and 200 Knots)

As we would expect, increasing the helicopter's speed makes the spiral smaller. The change in the spiral radius when increasing the speed from 50 to 100 knots is more significant than the change in the spiral radius when increasing the speed from 100 to 200 knots.

We now look at how the helicopter speed affects the number of dips and time to ensure detection (i.e., cover a total angle > 360 -degree). We expect the results to match what we saw with the spirals in Figure 7: fewer dips will be required for faster helicopters. This effect, however, is stronger at slower speeds, i.e., the slower the helicopter flies, the more we gain, in terms of number of dips needed, from accelerating. Figure 8 shows how number of dips and time to complete The 360-degree area of coverage will change when we vary the helicopter's speed.

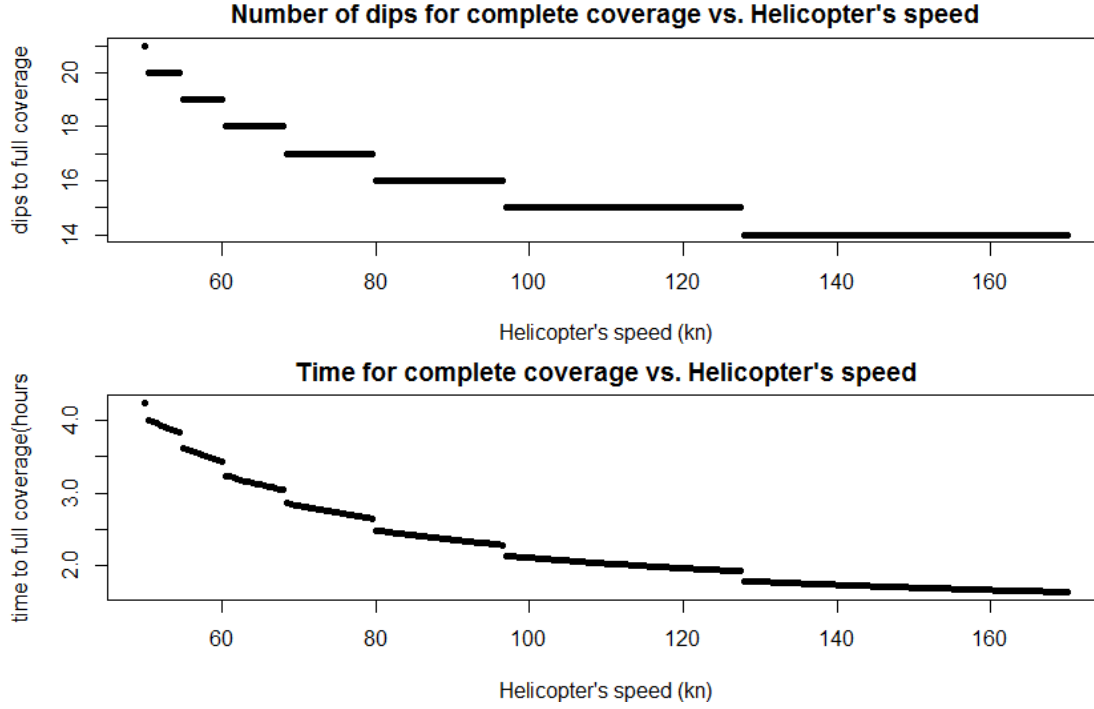


Figure 8. Number of Dips and Time to Complete Coverage vs. Helicopter's Speed

The results match what we expect, a decreasing marginal effect. The number of dips is a step function, i.e., we only see improvement when the speed is fast enough for the helicopter to need one less dip. On the other hand, the time function slightly improves when the speed increases, in a $time = \frac{dist}{speed}$ fashion, and “jumps” when we need one

less dip, saving the helicopter more time than just the time saved for flying faster. Note that if the helicopter's speed was infinite (and dipping time negligible) the helicopter would dip in a circle and not a spiral, creating a regular polygon, centered on the datum with sides of length $2 \times R$. The number of dips needed then would be

$$\frac{360}{2 * \sin^{-1}(\frac{R}{T_A * U})} = \frac{180}{\sin^{-1}(\frac{R}{T_A * U})} \quad (\text{see Figure 18}). \quad \text{With the parameters we used}$$

($R = 3, T_A = 1, U = 8$), that number is nine dips.

2. Arrival Time

We proceed with a similar analysis as we vary the arrival time of the helicopter to the AoU. First, we examine how varying the arrival time affects the spiral. Figure 9 shows arrival times of 30, 60, and 90 minutes ($V = 100, U = 8, R = 3, 5$ minutes per dip).

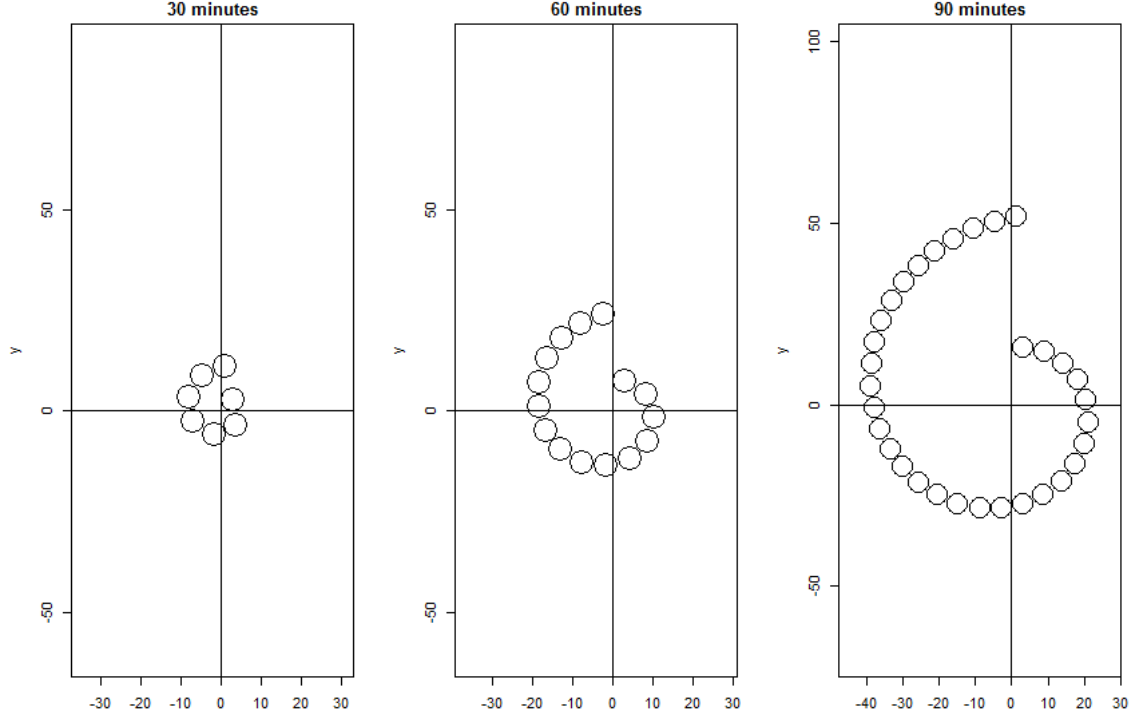


Figure 9. Spirals When Varying the Arrival Time (0.5, 1 and 1.5 Hours)

As expected, arriving later rather than earlier has a negative effect. This effect is very strong. The difference between arriving 30 minutes late, and an hour or two hours after the initial detection is very significant. This illustrates how important it is to arrive as quickly as possible to the datum and to start searching. We now look at the time and number of dips required for complete coverage, as shown in Figure 10.

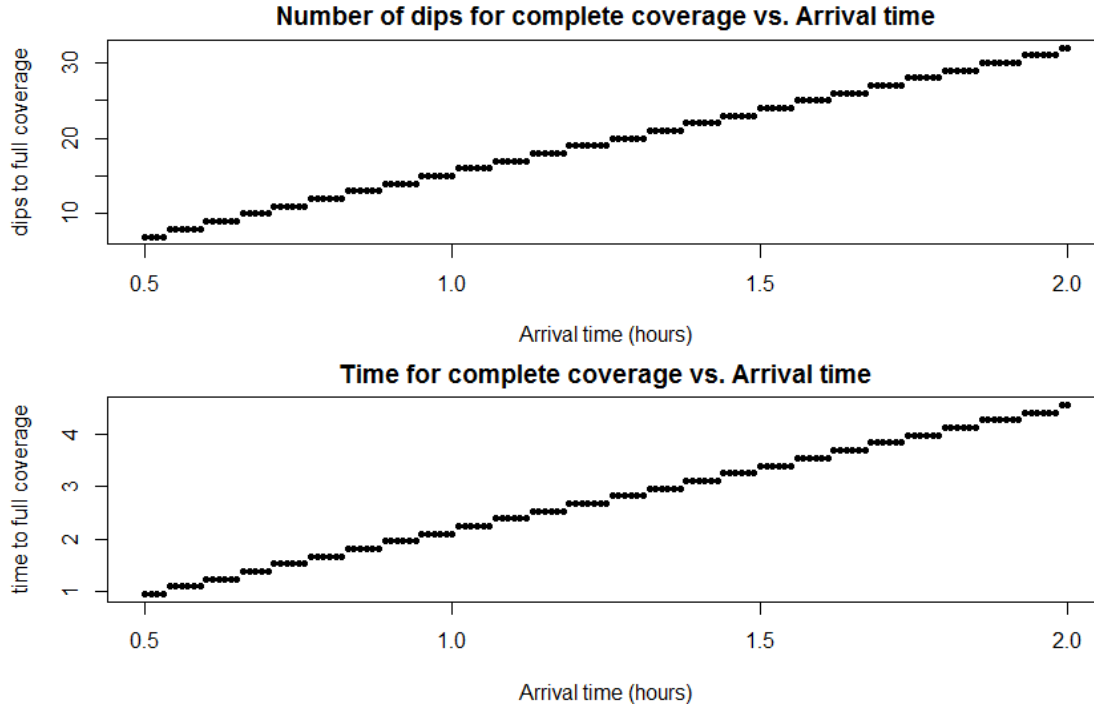


Figure 10. Number of Dips and Time to Complete Coverage vs. Arrival Time

When looking at Figure 10 we can see that both time and the number of dips grow linearly with respect to the arrival time to the datum. Some intuition about this linear relation is given in Chapter III.

3. Time per Dip

We now analyze the effect of dipping time. Dipping time impacts the results in two ways: 1) Direct—the longer the time it takes to dip, the longer it will take the helicopter to find the submarine; and 2) Indirect—longer dipping time gives the submarine more time to “run away,” making the next dip further away from the datum and thus less effective. Several factors may affect dipping time, including the gear used, crew proficiency, and uncertainty regarding the submarine’s depth. Figure 11 shows the dipping spirals for 2.5, 5, and 10 minutes per dip ($R = 3, T_A = 1, U = 8$).

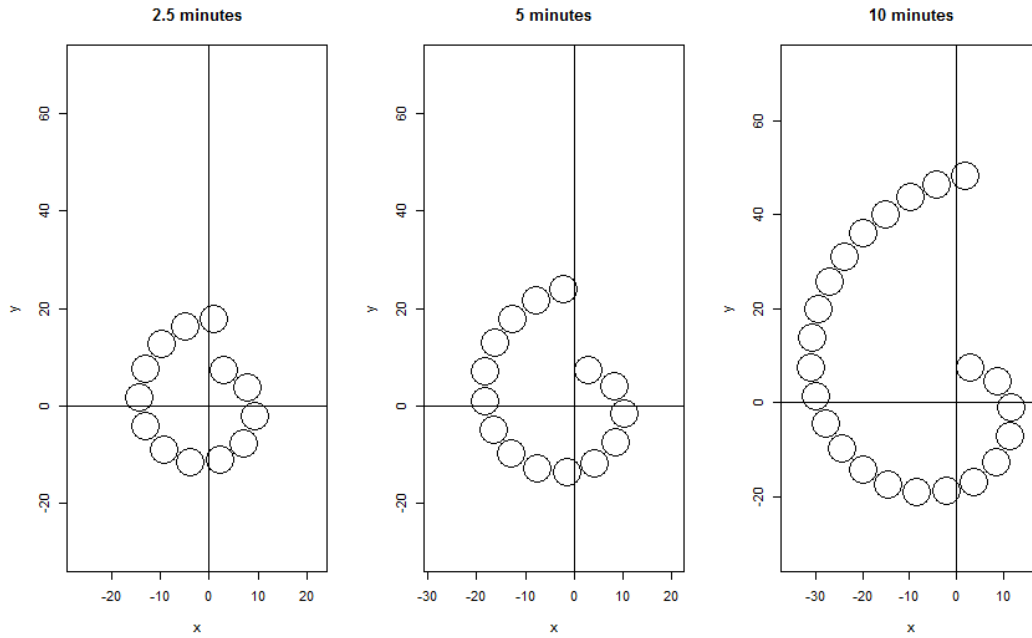


Figure 11. Spirals with Varying Dipping Times (2.5, 5 and 10 Minutes per Dip)

As we would expect, longer dipping time creates bigger spirals. Although we barely see a difference between 2.5 and 5 minute dips, we do see a significant change between 5 and 10 minute dips. We investigate this further by plotting the number of dips and time to complete coverage against the time per dip. The results appear in Figure 12.

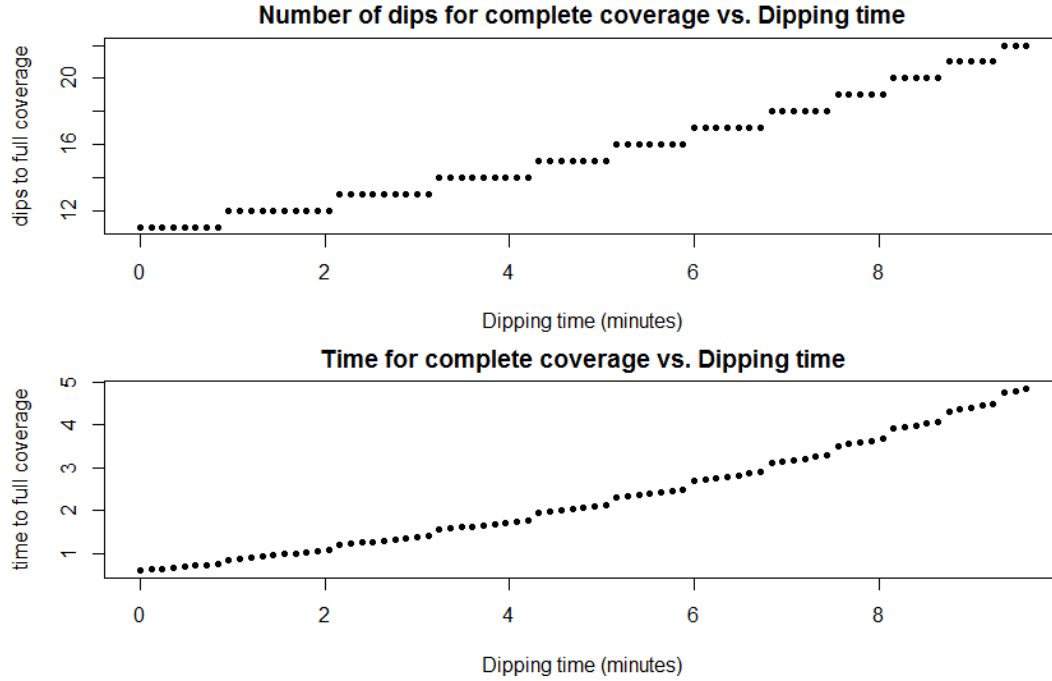


Figure 12. Number of Dips and Time to Complete Coverage vs. Time per Dip

We see that for fast dips (i.e., those less than 5 minutes) the relationship between time per dip and time to detection is almost linear. After that, slower dipping has an increasing effect on time and number of dips for complete coverage.

4. Dipper's Detection Range

We now analyze the effect of detection range. We note that this might be affected by weather and sea condition and that in order to actually improve this parameter, a more effective dipper must be acquired. As with the other parameters, we start with visually inspecting the spirals with a 1.5, 3, and 6 NM detection radius, respectively. The spirals appear in Figure 13 ($T_A = 1, U = 8, 5$ minutes per dip).

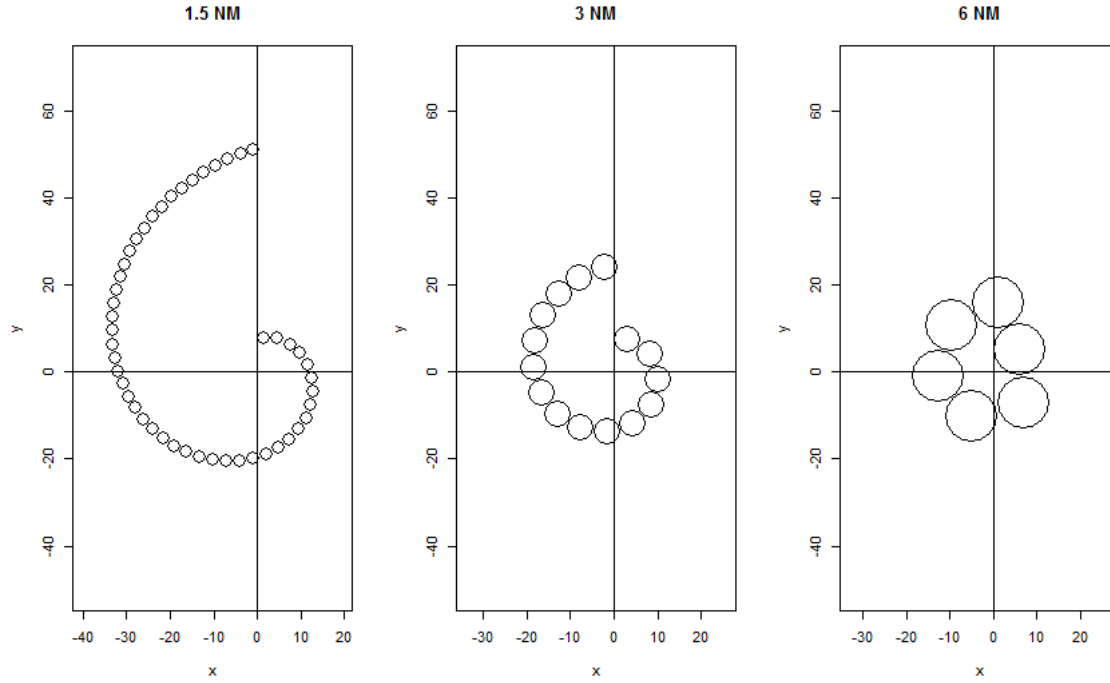


Figure 13. Spirals with Varying Detection Radii (1.5, 3, and 6 NM)

Figure 13 demonstrates a very significant effect: when we double (or halve) the detection radius, the dipping pattern changes considerably. We look at the number of dips and time to complete detection to understand the relationship better. We note that if the dipping time is negligible, the detection radius would have less impact, as the helicopter can just fly in a spiral and dip continuously. We plot the number of dips and time to complete coverage against the detection radius in Figure 14.

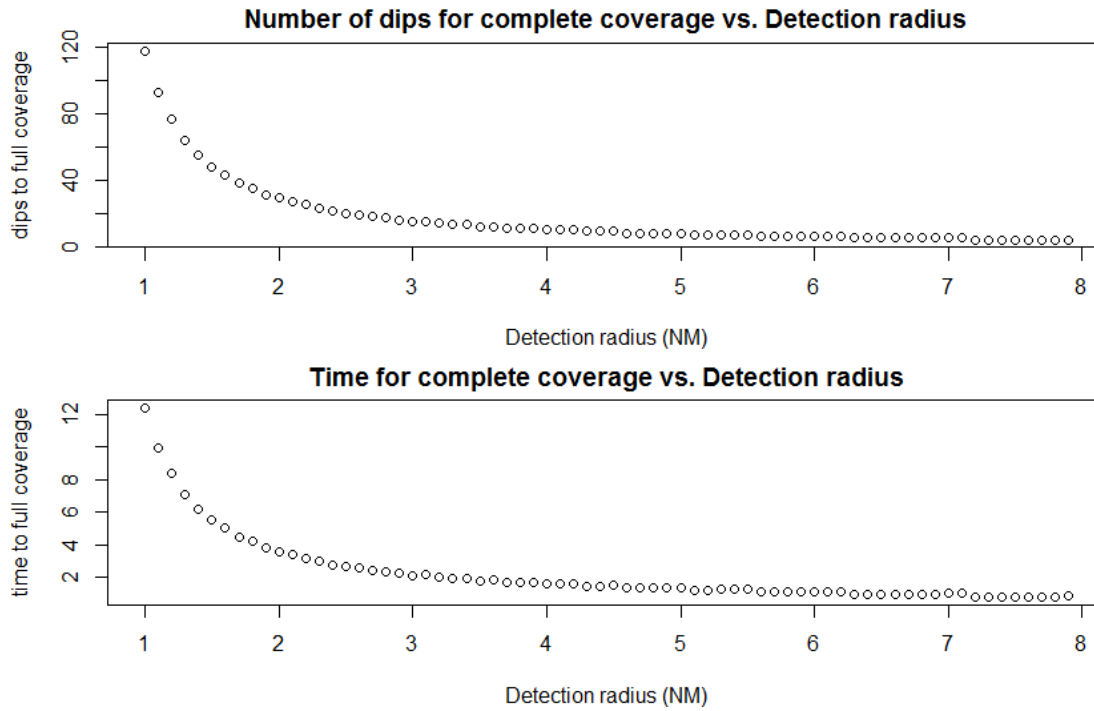


Figure 14. Number of Dips and Time to Complete Coverage vs. Detection Radius

We see that the detection radius has a very strong impact. If we zoom in on these figures, we also see some interesting dynamics. Figure 15 presents the zoomed-in view of these images.

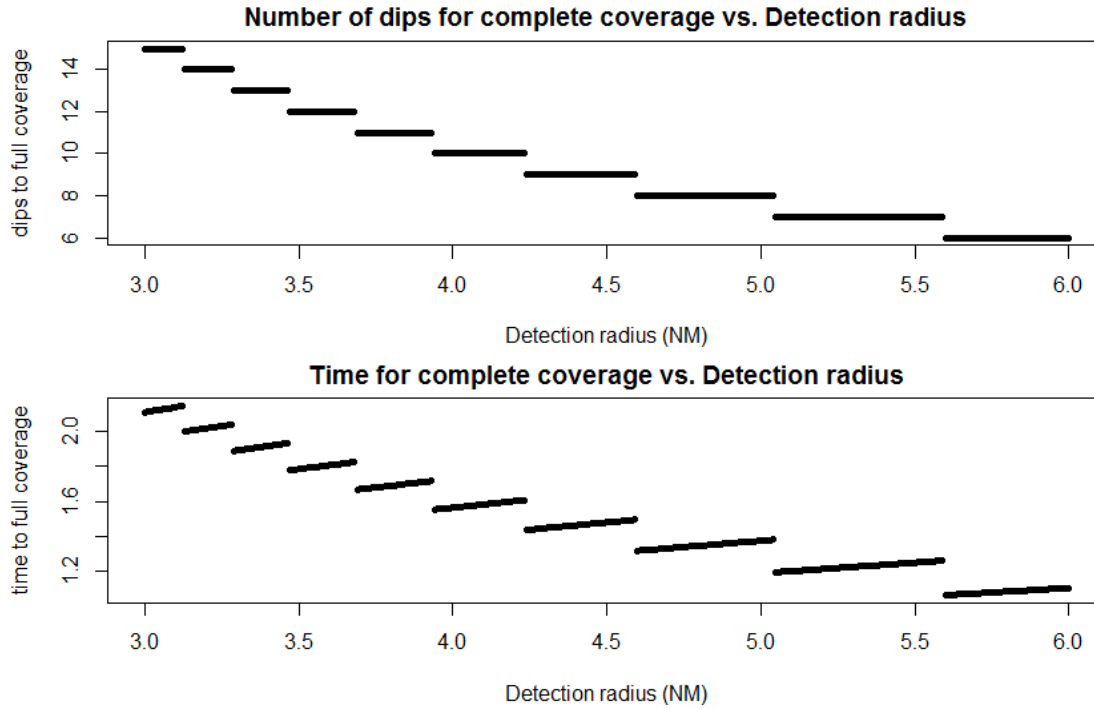


Figure 15. Zoom-in on Time and Dips for Complete Coverage vs. Detection Radius

There are two important observations. First, to significantly improve the search performance, we need to significantly increase the detection radius of the dipper. If the dipping technology only improves by 10 to 20 percent per generation, we may not see much difference in search performance until we move forward several generations. Second, there appears to be an abnormality where time until complete coverage increases with a slight increase in detection radius. This is easy to explain. When we increase our detection radius, we make our next dip further away, and it will take longer to get there. A larger radius results in better coverage. If it is only a slightly improved coverage, though, we may need to make the same number of dips as for the smaller radius. Since each dip takes longer, the actual time to complete the search increases with sensor radius until we reduce the number of dips. This results in a jump downwards in search time, as shown in Figure 15. We note that if we know that the helicopter can “cheat” by forcing overlaps between dips and then Figure 15 time to complete coverage would be a step function without the increasing parts.

5. Submarine's Speed

The last parameter we examine is the submarine's speed. The reason this is the last one is that we cannot control it in any way. We first look at the spirals corresponding to submarine speeds of 4, 8, and 16 knots, with a helicopter speed of 100 knots ($T_A = 1, R = 3$, 5 minutes per dip), as shown in Figure 16.

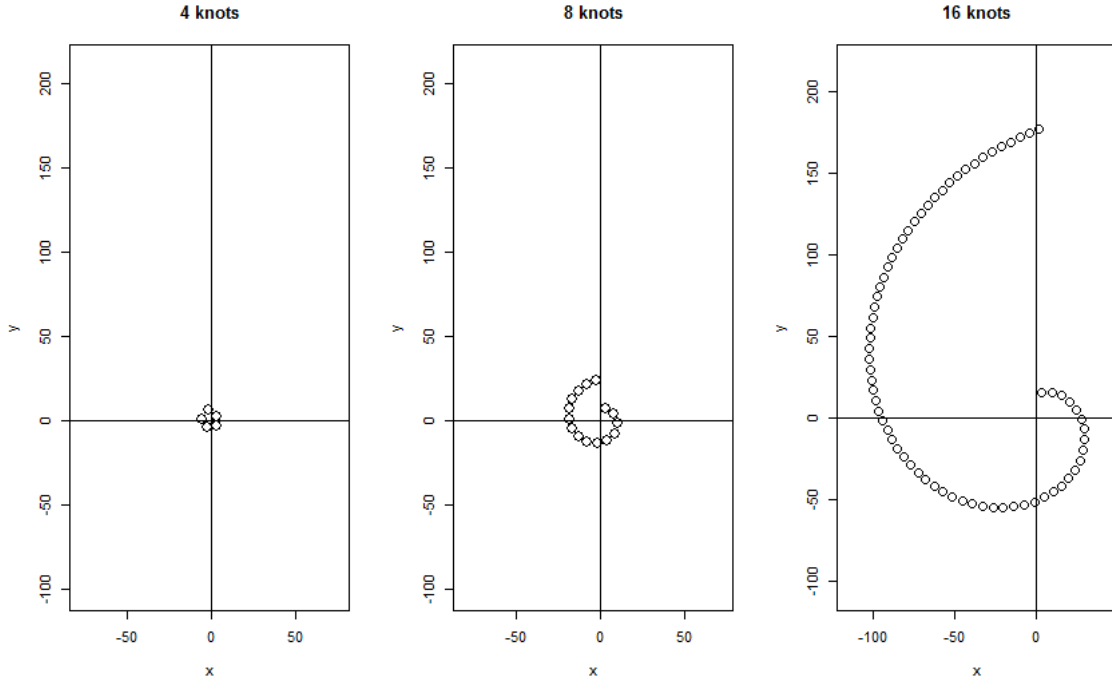


Figure 16. Spirals with Varying Submarine Speeds (4, 8, and 16 Knots)

We see that the submarine's speed has a very strong impact on the search spirals. There are two main reasons for this. First, the initial contact with the submarine occurs further away the faster the submarine moves, which affects the search time and number of dips (see subsection 2). Second, the helicopter must travel further between successive dips to keep up with a faster submarine. Figure 17 illustrates this effect.

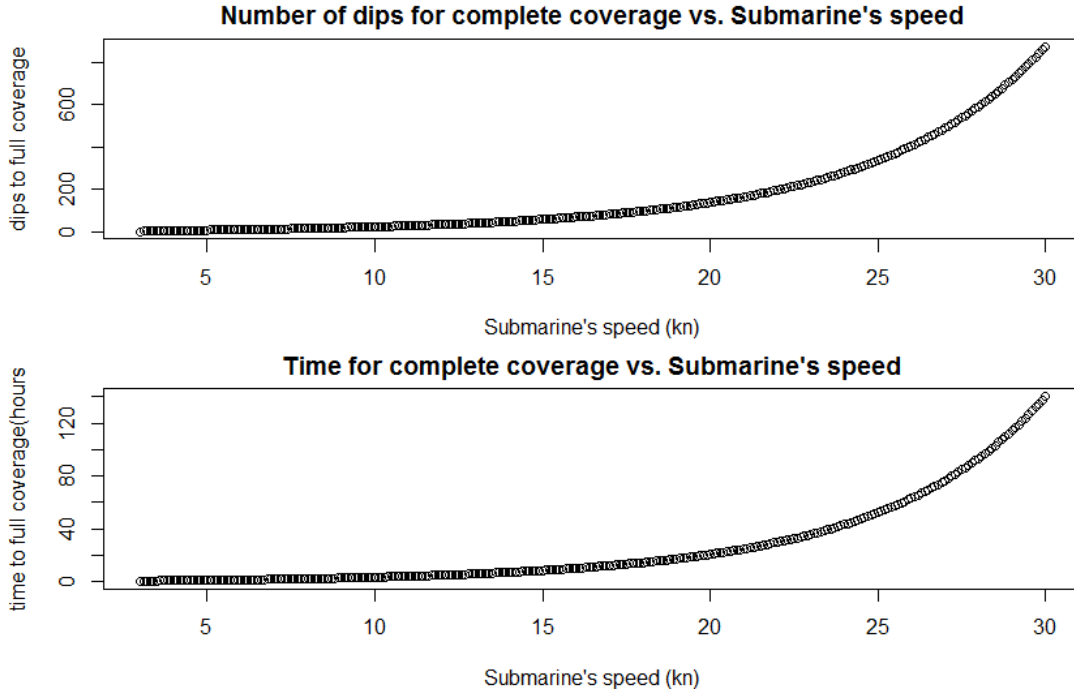


Figure 17. Time and Dips for Complete Coverage vs. Submarine's Speed

Now we can clearly see the differences between slow and fast submarines in terms of detection. While slow submarines (~8 knots) can be detected in a reasonable amount of time (i.e., an hour or two) and number of dips, faster submarines (according to open sources, modern submarines can travel as fast as 30 knots²) would take days to find, which is clearly not feasible.

D. PROOF OF THE OPTIMAL DIPPING PATTERN

There are several ways to define the best dipping pattern. We choose the optimal dipping pattern to be the one that, given a limited number of dips (because of limited flight endurance), maximizes the probability of detecting the submarine. Since we assume that we know the speed U of the submarine, the AoU at time T is a circumference of a circle with radius $T*U$; we call this C_T . Since the size of the circumference is growing with time, we look at the problem using coverage angles, as

² Wikipedia, s.v. "Underwater speed record," retrieved August 9, 2016, https://en.wikipedia.org/wiki/Underwater_speed_record

defined in Section A (subsection 12). Absent any knowledge regarding the bearing of the submarine, we assume any direction is equally likely, that is, the direction of the submarine is uniformly distributed between 0° and 360° . In each dip we calculate the coverage angle, α , such that $\sin(\alpha/2) = \frac{R}{T \times U}$. Figure 18 illustrates the logic behind this calculation.

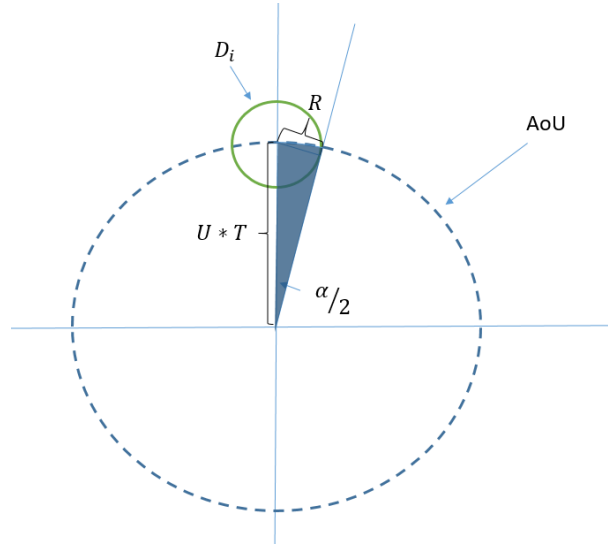


Figure 18. Calculation of Coverage Angle

Since we assume that the movement direction of the target is uniformly distributed, the probability of detection by a disjoint dip equals the coverage angle divided by 360. Therefore, a larger effective coverage angle is equivalent to a higher detection probability. The question is what is the optimal way to dip? We focus on a related question first. Given the current dip location, where should we dip next? We assert that Figure 19 illustrates the answer to this second question.

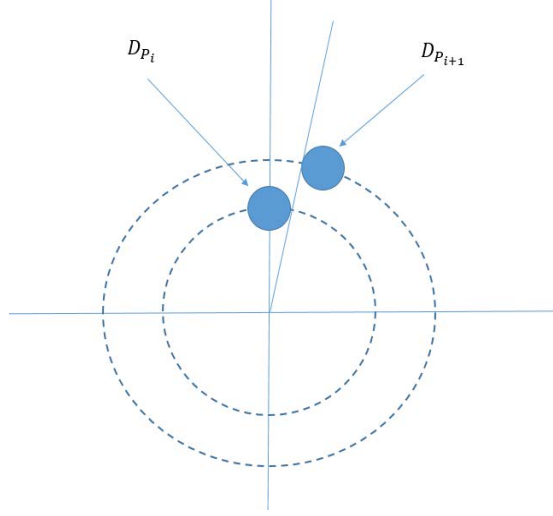


Figure 19. Optimal Next Dipping Location

Looking at Figure 19, we further assert that after dipping at point P_i the best next dipping point, P_{i+1} , would be a disjoint one. Moreover, point P_{i+1} is the closest possible disjoint dip; i.e., $D_{P_{i+1}}$ is tangent to the line that is tangent to D_{P_i} but “from the other side” (as shown in Figure 19). We prove this by contradiction.

We first make a few observations:

1. We assume that the helicopter does not get to the datum fast enough to find the submarine with one dip at the datum, i.e., $R < T_1 \times U$.
2. For each dip, we only need to choose the angle, rooted at the datum, with respect to the vertical axis, θ_{i+1} (or, equivalently, with respect to the previous dip, $\theta_{i+1} - \theta_i$). Note that the distance from the datum is uniquely determined by the submarine’s speed U and the time T from first detection. Consequently, specifying θ_{i+1} determines the actual dipping point.
3. Since we dip in a clockwise direction and without going back and forth, θ_i is a monotonically increasing series.
4. Since we only need to decide the angle, we look at $f(\omega)$ - the effective coverage of a dip as a function of the angle. ω is defined as $\omega_{i+1} = \theta_{i+1} - \theta_i$ which is the angle created by the previous dip, the datum, and the new dip, as illustrated in Figure 20.

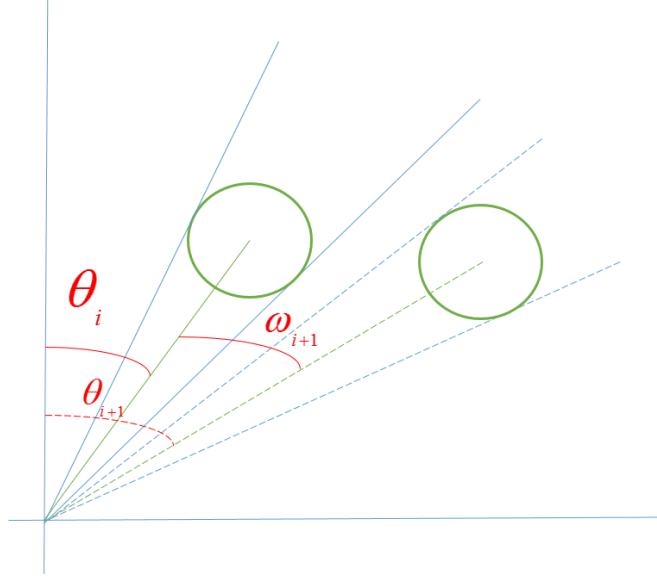


Figure 20. Definition of ω

5. $\omega_{i+1} = 0$ is then dipping again in P_i and therefore $f(0) = 0$, because dipping again in the same place will overlap entirely with the last dip.
6. T is a continuous function in ω . We use the cosine law as shown in Figure 21.

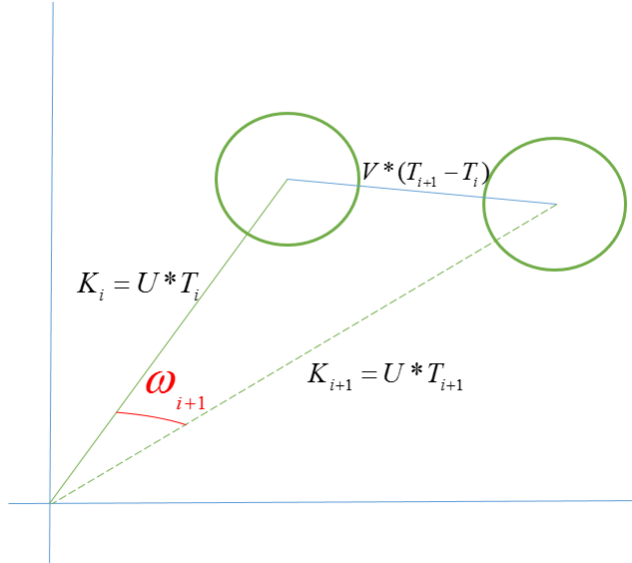


Figure 21. ω as a Function of T

We know the distance from the datum to the current dipping point, P_i , is $K_i = U \times T_i$ and that the distance from the datum to the next dipping point, P_{i+1} , is $K_{i+1} = U \times T_{i+1}$. We also know that the helicopter flies from P_i to P_{i+1} for time T_i to time T_{i+1} and therefore the distance from P_i to P_{i+1} is $V \times (T_{i+1} - T_i)$. Now using the cosine law (assuming $\omega < 180^\circ$), we can find the following relationship:

$$(V \times (T_{i+1} - T_i))^2 = (U \times T_i)^2 + (U \times T_{i+1})^2 - 2 \times U^2 \times T_i \times T_{i+1} \cos(\omega_{i+1}) \quad (2.1)$$

This shows us that T_{i+1} is a continuous function of ω_{i+1} . If there is a better place to dip than our proposed P_{i+1} , a point that covers a larger angular section, let us call it P_{i+1}^* , then it must be closer to the datum than P_{i+1} . This is because a point further away will not have any overlap with P_i (see Figure 5). Absent overlap (the dips are disjoint), we cover a smaller angle the further away we are from the datum.

7. Expanding on point 6, if such a point P_{i+1}^* exists, it is closer to the datum than P_{i+1} . This means it should take the helicopter less time to fly there, which means $\omega_{i+1}^* < \omega_{i+1}$ (solving Equation 2.1 for ω_{i+1} gives

$$(V \times (T_{i+1} - T_i))^2 = (U \times T_i)^2 + (U \times T_{i+1})^2 - 2 \times U^2 \times T_i \times T_{i+1} \cos(\omega_{i+1})$$

$$\omega_{i+1} = \cos^{-1} \left(\frac{(U \times T_i)^2 + (U \times T_{i+1})^2 - (V \times (T_{i+1} - T_i))^2}{2 \times U^2 \times T_i \times T_{i+1}} \right)$$

$$= \cos^{-1} \left(\left(1 - \frac{V^2}{U^2}\right) \times \left(\frac{T_i}{2 \times T_{i+1}} + \frac{T_{i+1}}{2 \times T_i} - 1\right) + 1 \right)$$

which is, for $T_{i+1} > T_i$, an increasing function in T_{i+1})

8. $f(\omega)$ is also a continuous function; to prove that, we now look at $f(\omega_i)$ the effective coverage of a dip, as defined before is

$$2 \times \sin^{-1} \left(\frac{R}{T_i \times U} \right) - \text{overlap}. \text{ Since } \frac{R}{T_i \times U} \text{ is always positive and less than 1,}$$

and T is a continuous function of ω , the first part is continuous. We now need to show that the overlap is a continuous function of ω . We recall that in the case of overlap and clockwise movement, the overlap is the angle between the left tangent to D_{i+1} and the right tangent to D_i , as shown in Figure 22.

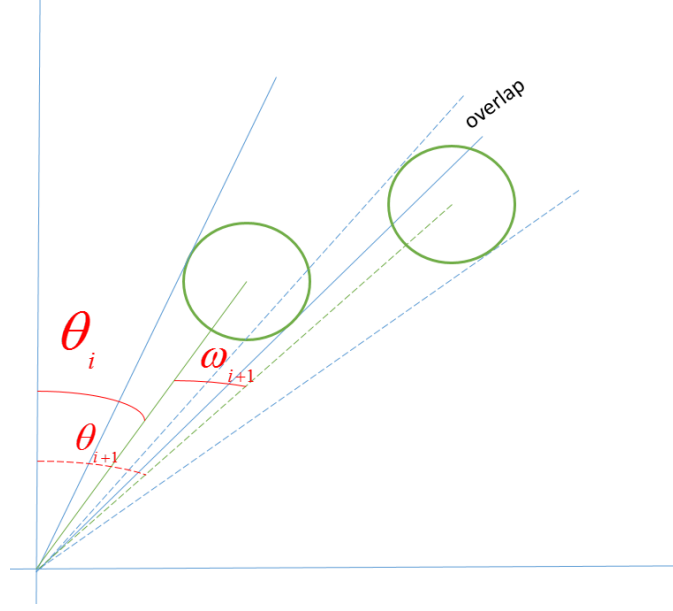


Figure 22. Overlap Calculation

The angle between the vertical axis and the right tangent to D_i can be expressed as $\theta_i + \sin^{-1}(\frac{R}{T_i \times U})$, and between the vertical axis to the left

tangent to D_{i+1} as $\theta_{i+1} - \sin^{-1}(\frac{R}{T_{i+1} \times U})$, the overlap can be expressed as

$$\theta_i + \sin^{-1}(\frac{R}{T_i \times U}) - \theta_{i+1} + \sin^{-1}(\frac{R}{T_{i+1} \times U}) = \theta_i - \theta_{i+1} + \sin^{-1}(\frac{R}{T_i \times U}) + \sin^{-1}(\frac{R}{T_{i+1} \times U})$$

which can be simplified to $-\omega_{i+1} + \sin^{-1}(\frac{R}{T_i \times U}) + \sin^{-1}(\frac{R}{T_{i+1} \times U})$. As

before, these are all continuous functions of T , and thus, this is a continuous function of ω .

We now turn to the proof itself. Let us assume that after dipping at point P_i , we determine there is a better place to dip than P_{i+1} . As mentioned before, we call the new suggested point P_{i+1}^* . P_{i+1}^* is closer to the datum and to P_i than P_{i+1} is, as explained in point 7.

If indeed P_{i+1}^* covers a larger angular section than P_{i+1} then there must exist a point P_j that is reachable by the helicopter in time to dip and that has the same effective coverage as P_{i+1} , as shown by the green circle in Figure 23.

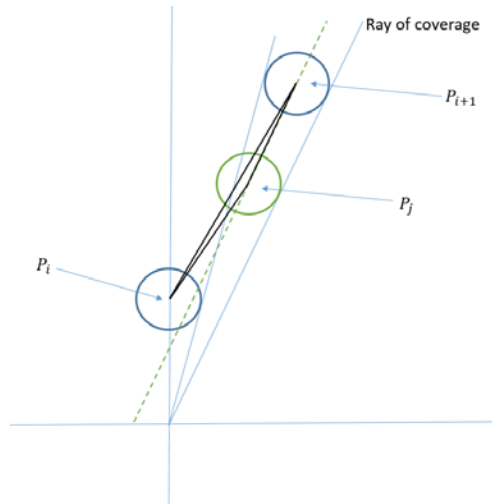


Figure 23. Proof by Contradiction

We prove this using the intermediate value theorem. As claimed in point 8, the effective coverage function is continuous. We have shown in point 5 that $f(0) = 0 < f(\omega_{i+1})$ (coverage cannot be negative), and we know that $f(\omega_{i+1}^*) > f(\omega_{i+1})$. Therefore, according to the intermediate value theorem, there is ω_j (and therefore P_j) for which $f(\omega_j) = f(\omega_{i+1})$ and $0 < \omega_j < \omega_{i+1}^*$, which means P_j is closer to our current dipping point, as explained in point 7. Figure 24 shows the idea graphically.

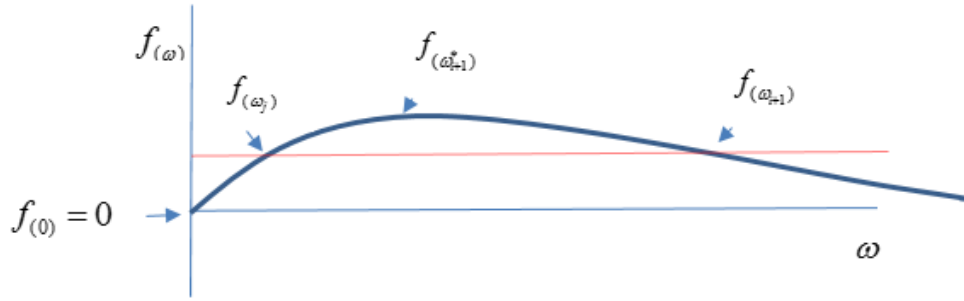


Figure 24. Intermediate Value Theorem

The angular coverage of D_j overlaps the angular coverage of D_i (because D_j is closer to D_i than D_{i+1}). Because of that, to be as good as D_{i+1} , i.e., to cover the same angle, D_{i+1} and D_j must both be tangent to the same ray from the datum. This is because the angle they cover, as explained earlier, is the angle created by the tangent to D_i and the tangent to themselves. We call this ray the “ray of coverage,” since it signifies how much those dips cover, and it can be seen in Figure 23. Because both D_{i+1} and D_j are tangent to the same line, and both have a radius of R , both P_{i+1} and P_j must lay on a line parallel to the “ray of coverage” and R (the dipping detection radius) away from it. That line is the green dotted line in Figure 23. We now show that assuming P_j exists leads to a contradiction. We first notice that $Dist_{i,i+1}$ is the shortest way from P_i to P_{i+1} since it is the distance of the straight line connecting the two points. We also note that $Dist_{i,i+1} = V \times \frac{K_{i+1} - K_i}{U}$, which is the distance the helicopter moves while the submarine moves between these two radii, and $Dist_{i,j} = V \times \frac{K_j - K_i}{U}$ is the distance the helicopter moves while the submarine moves between these two radii. We know that moving from P_j to P_{i+1} is parallel to the movement on the “ray of coverage” and therefore is the same length as the difference in the radii, meaning $Dist_{j,i+1} = K_{i+1} - K_j$. We can now see that

$$Dist_{i,j} + Dist_{j,i+1} = V \times \frac{K_j - K_i}{U} + (K_{i+1} - K_j) <$$

$$V \times \frac{K_j - K_i}{U} + V \times \frac{(K_{i+1} - K_j)}{U} = \frac{V}{U} [(K_j - K_i) - (K_{i+1} - K_j)] = \frac{V}{U} (K_j - K_i) = Dist_{i,i+1}. \quad (\text{The}$$

inequality part of the equation comes from the fact that $V > U$; the helicopter is faster than the submarine.) We found a path from P_i to P_{i+1} that is shorter than $Dist_{i,i+1}$, contradicting the fact that it is the shortest path. Since we only had one assumption, which was that point P_{i+1}^* exists and is a better point to dip than P_{i+1} , this assumption cannot be true. Therefore, such a point does not exist, and P_{i+1} is the optimal next dipping point.

E. TWO SPEEDS MODEL

We now relax one of our assumptions. We assume that instead of knowing the submarine exact speed, we have two options. The question we ask is whether we want to dip according to the slower speed first and then the faster one, or the other way around. To explain the difference, we present Figure 25.

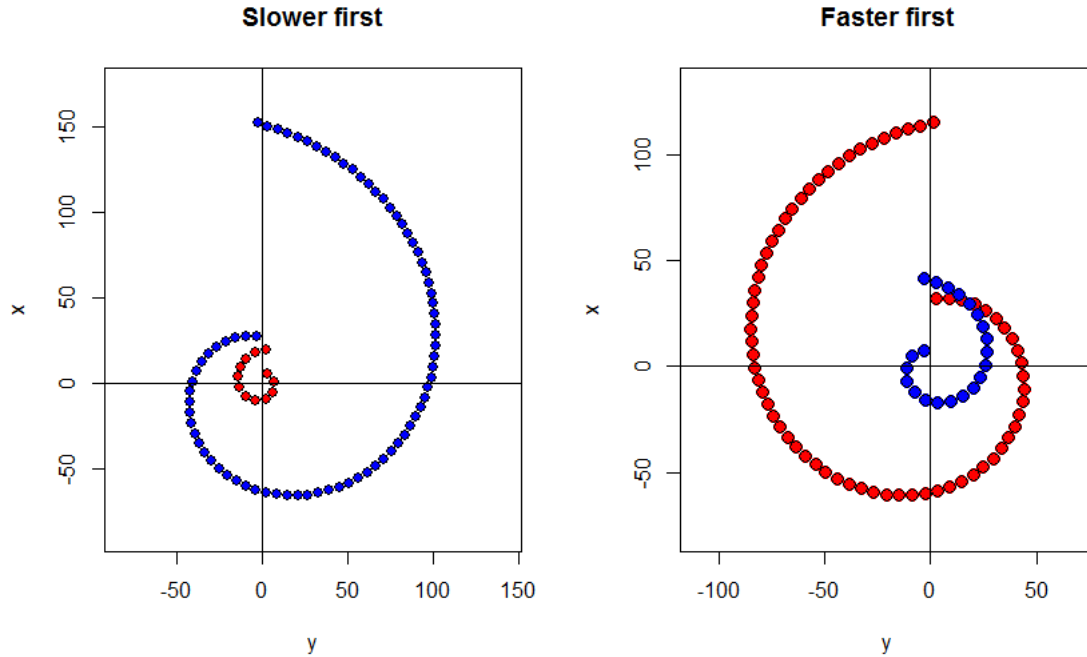


Figure 25. Two Speed Options for Dipping Patterns. Slower First (left) and Faster First (right)

In Figure 25, we illustrate the dipping pattern for the two cases: blue represents the dips corresponding to the submarine's faster speed, while the red represents those corresponding to the slower speed. In the left figure, we begin by dipping against the slower speed, then fly out and dip against the faster speed. In the right figure, we start by dipping against the faster speed, and then fly inward and dip against the slower speed.

Our measure of performance is the expected time to detection. We did not examine all of the parameters' effects on this problem but rather focused on the effect of the probabilities of the target moving in one speed or the other. Figure 26 shows how the expected time to detection changes when we vary the probability the target is moving with the faster speed (submarine's speeds are 5 and 8 knots).

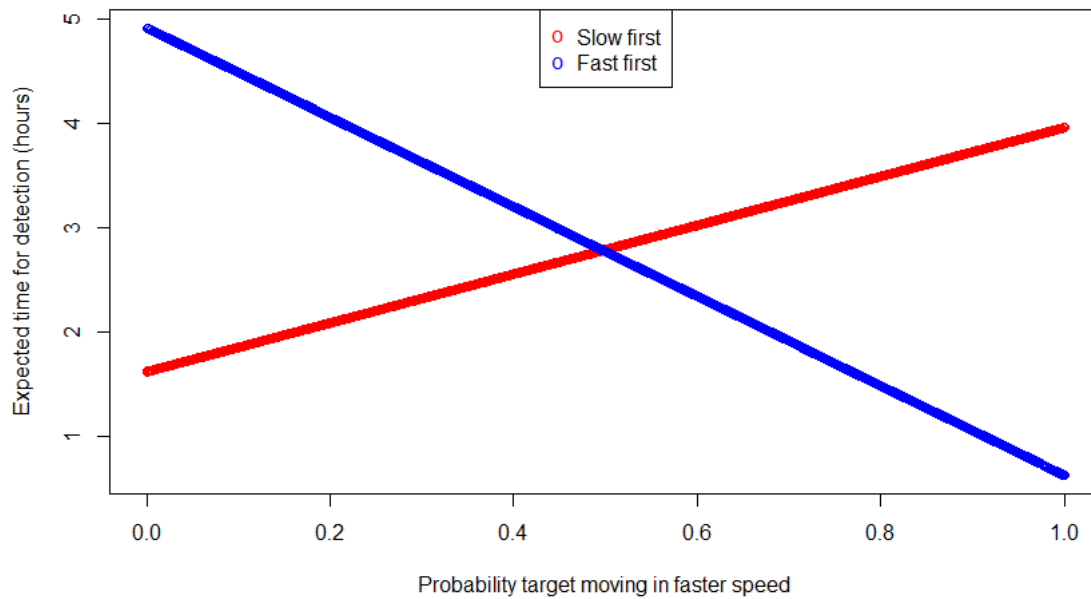


Figure 26. Two Speeds, Detection Time vs. Probability of Target Moving at Faster Speed

In blue, we see the expected time if we start by following the faster speed, and in red, the expected time to detection if we follow the slower speed first. As expected, the higher the probability the target is moving with its faster speed, the better it is to start with that by dipping according to that faster speed (blue line). We find that varying the

problem parameters affects the expected time for detection. Yet, it did not have a significant effect on the “switching point,” the probability for which the two dipping orders (fast-slow and slow-fast) have the same expected time. This probability is around 50 percent regardless of the parameters. For larger speed differences between the fast and slow submarine speed (>5 knots) the switching point is a bit over 50 percent ($\sim 50.5\%$), while for smaller differences (1 to 2 knots), it is slightly less than 50 percent ($\sim 49.5\%$). We note that if we look at these results from a game theory approach, the optimal mixed strategy for both the submarine and the helicopter is a 50–50 strategy.

F. BUOYS

There are four main differences between buoys and a dipper. Since this chapter addresses a helicopter equipped with a dipper, we consider those differences to see what effect they might have. Those differences include the following:

1. Time per dip—while it takes some time to dip, it should take less time when deploying a sonobuoy.
2. Detection radius—the dipper is stronger and therefore has a larger detection radius.
3. Buoys cover the area continuously (i.e., they are left in the water) while a dipper stops detecting once it is pulled out of the water.
4. The helicopter is limited in the number of buoys it can carry.

We start by examining the first two differences. To do that we examine the trade-off between dipping time and detection radius by varying both and watching the effect they have on time to full coverage. The results appear in Figure 27.

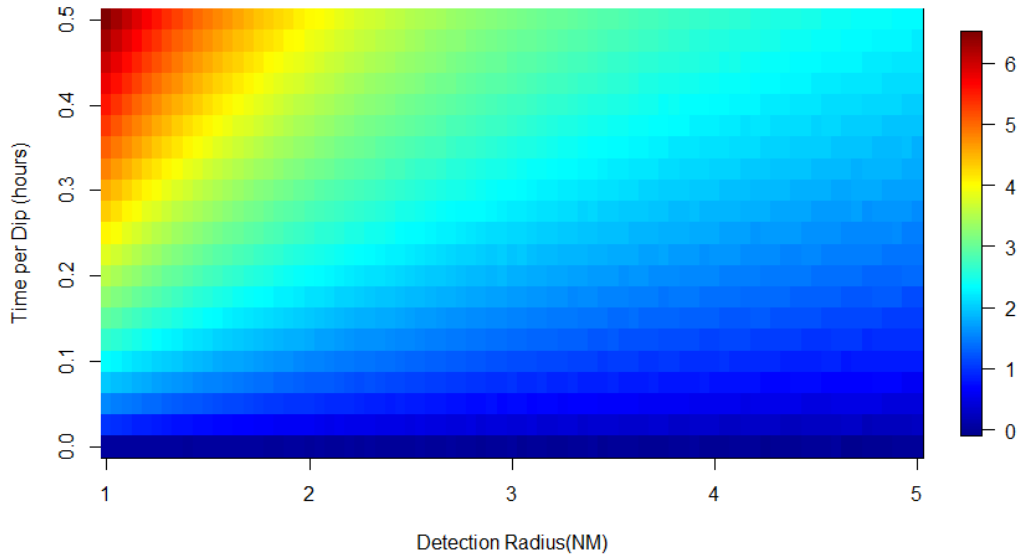


Figure 27. Comparing Detection Radius and Dipping Time, Showing the Log of Time to Complete Coverage

In Figure 27, we plot the log of time to complete coverage when we vary the detection radius and the time per dip. We chose to plot the log and not time itself so that the differences would be clearer. Points that have the same color in the figure are equally effective, so for example a dipper with 4 NM detection range and 0.4 hours per dip is equivalent to one with 2 NM range and 0.15 hour per dip (complete coverage in ~4 hours). A buoy with 1 NM detection radius and 0 time per dip is roughly equivalent to a dipper with 3 NM range and 0.1 hours (6 minutes) time per dip (complete coverage in ~1 hour).

We now examine the effect of leaving the buoys in the water. Leaving the buoys in the water allows detection to occur when the target passes in the detection area even if the helicopter has left the vicinity. This cannot occur with a dipper; the helicopter and dipper must be co-located for a detection to occur. If we know the target's speed, this persistence effect of the buoys does not matter; the helicopter dips in only the moment the target could be at that location. A buoy would be equally effective in this situation. By contrast, if we do not know the target's speed, the persistence effect of the buoys may play a more significant role. We assume the target speed is uniformly distributed between

a slow and a fast speed. The AoU then becomes a donut shape, and when placing a buoy, we need to decide how far away from the datum to place it. Figure 28 illustrates this.

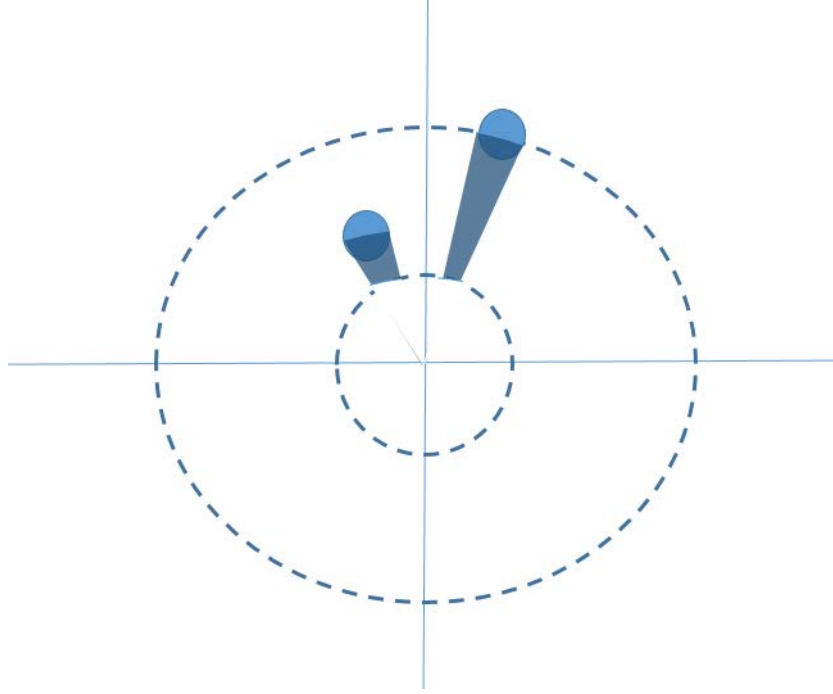


Figure 28. Buoy Placement

The dotted lines represent the slow and fast speeds. The two filled circles represent possible locations to place the buoy, and the highlighted area represents the covered area. Since the buoy stays in the water, the covered area includes all locations that will lead the submarine into the buoy's range, even in the future. Placing the buoy closer to the datum gives us a wider angle, while placing it further away gives us a wider range of speeds covered. The coverage of a buoy in this case is given by the equation:

$$\frac{\sin^{-1}\left(\frac{R_{\text{det}}}{X}\right)}{\pi} \times \frac{\min(1, X - T \times U_{\text{slow}})}{T \times (U_{\text{fast}} - U_{\text{slow}})} \text{ where } X \text{ is the distance of the buoy from the datum.}$$

This function has its maximum at $X = T \times U_{\text{fast}}$, which is placing the buoy on the outer ring. Since we now know we want to place the buoy on the outer ring, we only need to

consider the faster speed of the submarine, which brings us to the same model we developed for the dipper scenario.

The limited number of buoys does not affect the optimality of our model, but should be taken into consideration when using our model.

THIS PAGE INTENTIONALLY LEFT BLANK

III. NON-UNIFORM DIRECTION

In Chapter II we assumed that the direction in which the submarine moves is uniformly distributed between 0 and 360 degrees. In this chapter, we relax that assumption to consider the situation where the searcher has some knowledge about the submarine's movement direction. As in Chapter II, we assume that the speed is still constant and known. We consider three models that capture this additional knowledge: (a) a three rays model, (b) a five rays model, and (c) a three wedges model.

A. THREE RAYS MODEL

The first model we present is a three rays model. It is a simple discrete submarine's movement direction model, but there are interesting insights we get from looking at it.

1. Model Description

We begin by examining a very basic case. The submarine is moving away from the datum in a known constant speed, along one of three possible rays. Each of the side rays creates an angle θ with respect to the center ray. The right, center, and left rays are selected by the submarines with probabilities q , p , and $1 - p - q$, respectively. See Figure 29.

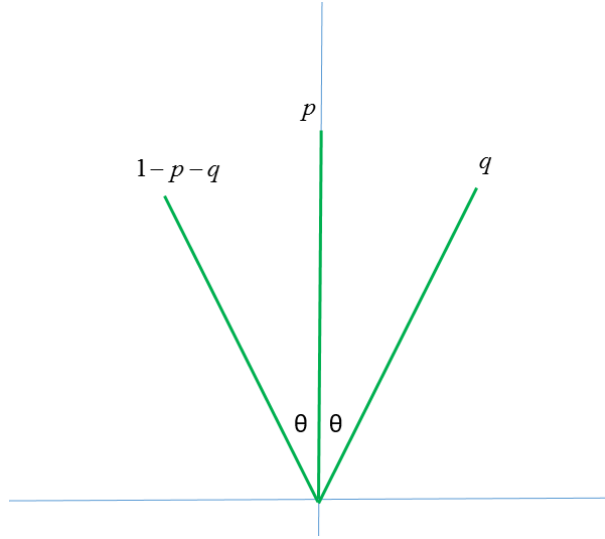


Figure 29. Three Rays Model

a. Notation

In this model, we use the following notation:

- U —submarine's speed
- V —speed of the search helicopter
- $S = \frac{V}{U}$ —the ratio between the helicopter's speed and the submarine's speed
- p —probability the submarine is moving along the center ray
- q —probability the submarine is moving along the right ray
- θ —angle between rays
- T_1 — time of the first dip
- T_l, T_c, T_r —dipping time at the left, center, and right rays, respectively
- P_l, P_c, P_r —probability the target moves along left, center, and right side ray, respectively. $P_l = 1 - p - q$, $P_c = p$, $P_r = q$

b. Model Description

In this scenario, we wish to minimize the expected time to detection. Since we know the submarine's speed, we only need to dip once along each ray—at the right time. Thus, we only need to decide the order in which the helicopter dips, such that the expected time to detection as shown in Equation 3.1 is minimized.

$$T_l \times (1 - q - p) + T_c \times p + T_r \times q \quad (3.1)$$

Intuitively, one might dip according to the likelihood the submarine is on a certain ray, starting at the ray with highest probability. The problem with this strategy is that the helicopter may have to “jump” over rays and therefore waste time flying back and forth.

By controlling the dipping order, we control the time in which we dip along each ray. To find the expected time to detection we need to calculate the T_i 's for a given dipping order. In particular, we need to answer the following question: Given that the helicopter dipped at a certain ray, when and where will it dip along another ray such that the dip will coincide with the presence of the submarine at the new dipping point had it selected that ray? This is shown in Figure 30.

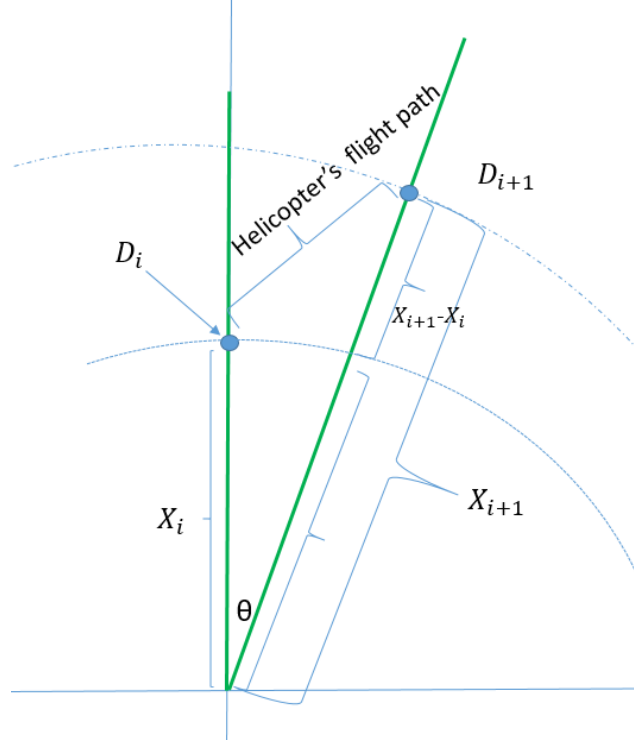


Figure 30. Flight between Rays

If at time 0 the helicopter dips at point D_i on the vertical ray, which is a distance X_i away from the datum. The new dipping point, D_{i+1} , which is a distance X_{i+1} from the datum, is on the intersection of the diagonal ray θ degrees away from the vertical ray and the location circumference of the submarine at time $\frac{X_{i+1} - X_i}{U}$. For this to happen the submarine needs to move $X_{i+1} - X_i$ and the helicopter needs to fly $\sqrt{X_i^2 + X_{i+1}^2 - 2 \times X_i \times X_{i+1} \times \cos(\theta)}$. Since we know the speeds of both the submarine and the helicopter, and we know the helicopter would fly in a straight line to the next point (the fastest way), and they need to move these distances in the same time, we can find X_{i+1} from the following equation: $\sqrt{X_i^2 + X_{i+1}^2 - 2 \times X_i \times X_{i+1} \times \cos(\theta)} / V = (X_{i+1} - X_i) / U$. Solving this gives the following solution (remembering that $S = \frac{V}{U}$):

$$X_{i+1} = X_i \times \frac{S^2 - \cos(\theta) + \sqrt{\cos(\theta) * (\cos(\theta) - 2 \times S^2) + 2 \times S^2 - 1}}{S^2 - 1}.$$

Define $f_{S,\theta} = \frac{S^2 - \cos(\theta) + \sqrt{\cos(\theta) \times (\cos(\theta) - 2 \times S^2) + 2 \times S^2 - 1}}{S^2 - 1}$ and we get that

$$X_{i+1} = X_i \times f_{S,\theta}.$$

After finding the dipping distance, we know that the dipping time is $\frac{X_{i+1}}{U}$ (since the submarine is moving in a constant speed and direction). The dipping time is therefore

$$T_{i+1} = \frac{X_{i+1}}{U} = \frac{X_i \times f_{S,\theta}}{U} = T_i \times f_{S,\theta}.$$

There are six possible dipping patterns:

1. $l \rightarrow c \rightarrow r$
2. $l \rightarrow r \rightarrow c$
3. $c \rightarrow l \rightarrow r$
4. $c \rightarrow r \rightarrow l$
5. $r \rightarrow l \rightarrow c$
6. $r \rightarrow c \rightarrow l$

The expected time for detection for each pattern is calculated from Equation 3.1. For example, for pattern 1:

$T_l = T_1$, $T_c = T_l \times f_{S,\theta} = T_1 \times f_{S,\theta}$, $T_r = T_c \times f_{S,\theta} = T_1 \times f_{S,\theta}^2$ and the expected time to detection is $E_{\text{detection}} = T_l \times P_l + T_c \times P_c + T_r \times P_r = T_1 \times (1 - p - q) + T_1 \times f_{S,\theta} \times p + T_1 \times f_{S,\theta}^2 \times q = T_1 \times ((1 - p - q) + f_{S,\theta} \times p + f_{S,\theta}^2 \times q)$. We calculate the expected time of detection for each pattern:

1. $l \rightarrow c \rightarrow r: T_1 \times ((1 - p - q) + f_{S,\theta} \times p + f_{S,\theta}^2 \times q)$
2. $l \rightarrow r \rightarrow c: T_1 \times ((1 - p - q) + f_{S,2\theta} \times q + f_{S,\theta} \times f_{S,2\theta} \times p)$
3. $c \rightarrow l \rightarrow r: T_1 \times (p + f_{S,\theta} \times (1 - p - q) + f_{S,2\theta} \times f_{S,\theta} \times q)$

4. $c \rightarrow r \rightarrow l: T_1 \times (p + f_{S,\theta} \times q + f_{S,2\theta} \times f_{S,\theta} \times (1 - p - q))$
5. $r \rightarrow l \rightarrow c: T_1 \times (q + f_{S,2\theta} \times (1 - p - q) + f_{S,\theta} \times f_{S,2\theta} \times p)$
6. $r \rightarrow c \rightarrow l: T_1 \times (q + f_{S,\theta} \times p + f_{S,\theta}^2 \times (1 - p - q))$

The expected time to detection for a given pattern is a function of T_1 , S , θ , p and q . We can find, for any set of parameters values, the best pattern. We also note that the expected time has a linear relation to the arrival time. We noticed this effect in Chapter II, and even though the two models—the uniform and continuous in Chapter II and the discrete and non-uniform here—are different, the underlying movement equations of the submarine and helicopter are similar, and the linear relation remains.

2. Model Results

As explained before, there are five parameters in the calculation of the expected time for detection in each dipping pattern, but only four of them affect the choice of pattern. These factors are:

1. S —the ratio between the helicopter and submarine speeds.
2. θ —the angle between the rays.
3. p —probability the submarine is moving along the center ray.
4. q —the probability the submarine is moving along the right ray.

T_1 is not in the list because even though it affects the expected time to detection, it is a common multiplication factor in all of the six patterns. We use $p-q$ plots to graphically show results. Each plot corresponds to certain values of the relative speed S and the angle θ . An example plot is shown in Figure 31.

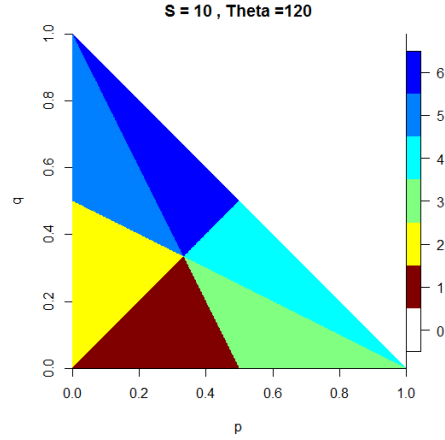


Figure 31. Three Rays, $S = 10$, $\theta = 120^\circ$

The interpretation of Figure 31 is as follows. The white region above the diagonal (numbered 0) represents the infeasible region where $p + q > 1$. The other colors code dipping patterns, representing the best dipping pattern for the corresponding values of p and q . Each color translates to a number according to the legend to the right. These numbers represent the dipping patterns in the same order in which they are listed in the model description. For example, the red region (1) corresponds to the pattern $l \rightarrow c \rightarrow r$. Since the angle used in Figure 31 is $\theta = 120^\circ$, the scenario is directionally symmetric. It is, in fact, a discrete version of the uniform scenario described in Chapter II, and therefore, we would expect that for $p = q = 1/3$ any one of the six dipping patterns will be equally effective. The helicopter will always choose the shortest way to the next ray, and will only fly over the third ray if needed. Therefore, in this case the order of visiting the rays does not matter. This point can be seen in the middle of the plot, where all colors intersect, as expected. We can see that when p grows, patterns 3 and 4 become dominant. These are the patterns that begin with dipping in the center ray. When q grows, patterns 5 and 6, which start at the right ray, become dominant.

Next, we study how S and θ affect the optimal dipping pattern. First, we fix θ at 90° and examine how S affects the dipping pattern. The results appear in Figure 32.

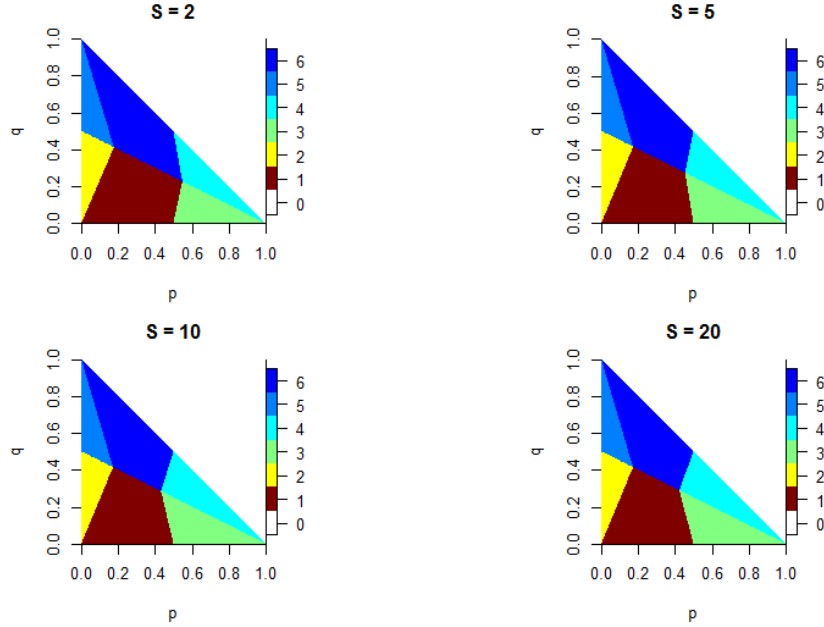


Figure 32. Three Rays, $\theta = 90^\circ$ Different Values of S

Note that the general layout of the regions of optimal pattern in Figure 32 are quite similar for the four values of S . We see, however, that by increasing the helicopter's speed, patterns 3 and 4 are more prevalent compared to patterns 1 and 6, which translates into more likely first dip in the center ray.

We next see what happens when we change the angle and keep the speed ratio constant. This time we set the speed ratio at $S = 10$ and vary the angle. The results appear in Figure 33.

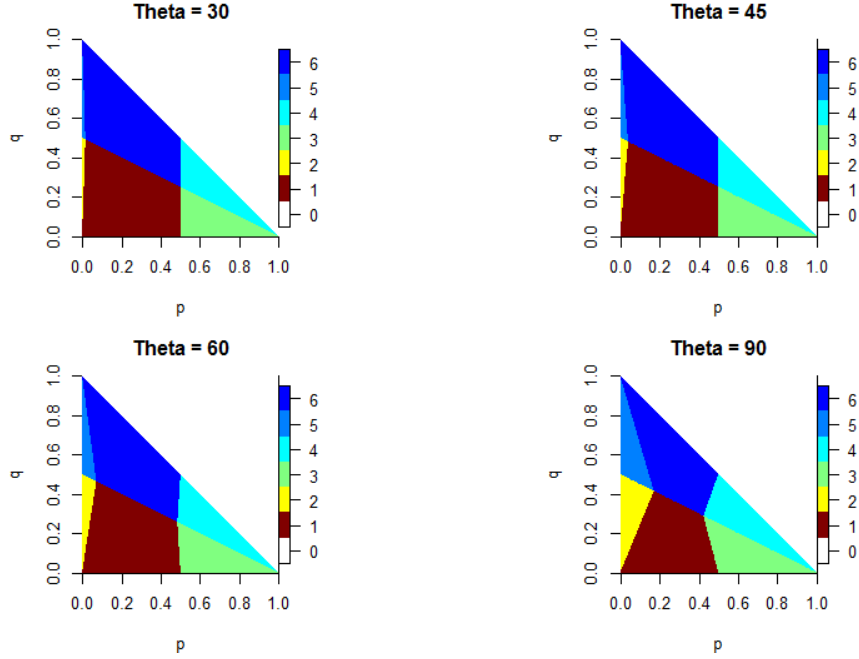


Figure 33. Three rays, $S = 10$, Varying Angle

We see that when the angle increases, patterns 2, 3, 4, and 5 become more likely than patterns 1 and 6. This implies that the bigger the angle is, the less likely we are to dip without jumping, and the more likely we are to either start in the middle or jump from left to right and keep the center ray for the last dip. This is slightly surprising, as we would expect the “penalty” for jumping over rays to increase as the angle increases and therefore patterns 1 and 6 to become more likely. To understand this, we need to look into the equations that govern the dipping patterns. Consider areas 1 (brown) and 2 (yellow). The line between areas 1 and 2 (the line for which all points to the right and down are in area 1 and up and left are area 2) can be found by comparing the expected times of both patterns (as explained in Section B of this chapter) to be

$$q = \frac{f_{S,\theta} - f_{S,\theta} \times f_{S,2\theta}}{f_{S,2\theta} - f_{S,\theta}^2} * p. \text{ This line always passes through the point (0,0), and its slope}$$

determines whether pattern 1 or 2 is dominating. As we can see, the slope is a complicated function of $f_{S,\theta}$ and $f_{S,2\theta}$, and intuition about these functions is not as straightforward as we would expect.

B. FIVE RAYS MODEL

We now expand the three rays model into five rays and examine the same parameters as in the three rays case.

1. Model Description

In the five rays model we have five rays, separated by an angle θ (the same angle for each of the two adjacent rays). The probability the submarine is moving along the center ray is p , along each one of the two adjacent “mid-rays” q , and along each one of the two side-rays $\frac{1-p-2q}{2}$, as shown in Figure 34.

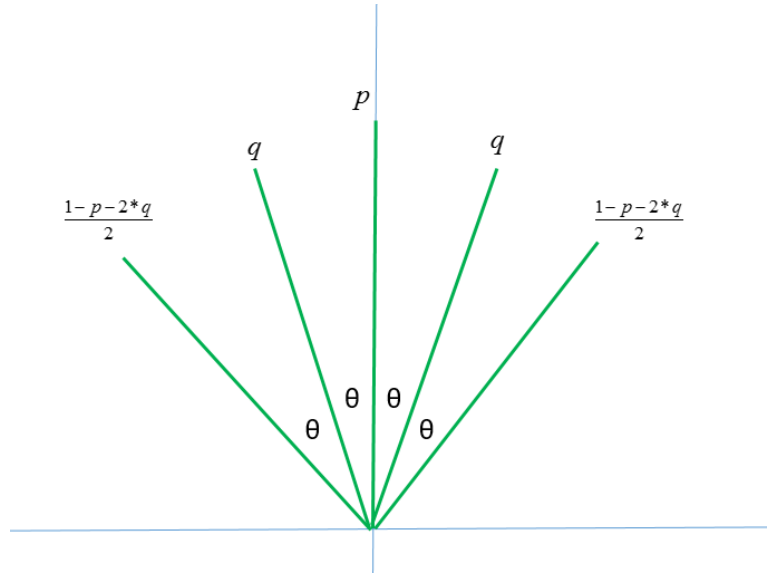


Figure 34. Five Rays Model

There are many more optional dipping orders when looking at the five rays model as compared to the three rays one. To reduce the complexity of the problem, yet keeping it realistic we add two assumptions: 1) $4 \times \theta < 180^\circ$, which means we know the general direction of movement of the submarine, and 2) $p > q > \frac{1-p-2q}{2}$, which means that the submarine is most likely to be closer to the center ray than to the side ones. This models the operational situation in which we have an estimated bearing, but it might be

slightly off. We keep the notation (from Sections A and B of this chapter) regarding the ratio between speeds and $f_{s,\theta}$ to calculate the time it takes to fly to the next ray after a dip (see Figure 30). We note that in the five rays model, in addition to the coefficients, $f_{s,\theta}$ and $f_{s,2\theta}$, we might need to use $f_{s,3\theta}$ and even $f_{s,4\theta}$, which are the relevant coefficients for the case where we jump over two or three rays. We denote t_{ll}, t_l, t_c, t_r and t_{rr} for the dipping times at each ray from left to right, respectively. As in the three rays model, we present the results $p-q$ plots. In the five rays model there are theoretically $5!=120$ dipping patterns, but our assumptions eliminate some patterns. Because the probabilities of the rays are symmetrical, we can look at only half of the combinations. Also, since $p > q > \frac{1-p-2 \times q}{2}$ more dipping patterns can be eliminated since we know (from the three rays model) that the only reason to “jump” over a ray is to get to another with higher probability. Thus, we end up with the following six possible dipping patterns that need analysis. The serial number of a pattern (order of dips) corresponds to the color scheme in the plots:

1. $rr \rightarrow r \rightarrow c \rightarrow l \rightarrow ll$ (right to left)
2. $r \rightarrow c \rightarrow l \rightarrow ll \rightarrow rr$
3. $r \rightarrow c \rightarrow rr \rightarrow l \rightarrow ll$
4. $r \rightarrow rr \rightarrow c \rightarrow l \rightarrow ll$
5. $c \rightarrow r \rightarrow l \rightarrow ll \rightarrow rr$
6. $c \rightarrow r \rightarrow rr \rightarrow l \rightarrow ll$

The corresponding expected times to detection are calculated in the same manner as in the three rays model. The expected times to detection for the various dipping patterns are:

$$\begin{aligned}
 1) \quad T_1 &\times \left(\frac{1-p-2 \times q}{2} \times (1 + f_{s,\theta}^4) + q \times (f_{s,\theta} + f_{s,\theta}^3) + p \times f_{s,\theta}^2 \right) \\
 2) \quad T_1 &\times \left(\frac{1-p-2 \times q}{2} \times (f_{s,\theta}^3 \times f_{s,4\theta} + f_{s,\theta}^3) + q \times (1 + f_{s,\theta}^2) + p \times f_{s,\theta} \right)
 \end{aligned}$$

$$\begin{aligned}
3) \quad & T_1 \times \left(\frac{1-p-2 \times q}{2} \times (f_{S,\theta} \times f_{S,2\theta} + f_{S,\theta} \times f_{S,2\theta} \times f_{S,3\theta} \times f_{S,4\theta}) + q \times (1 + f_{S,\theta} \times f_{S,2\theta} \times f_{S,3\theta}) + p \times f_{S,\theta} \right) \\
& T_1 \times \left(\frac{1-p-2 \times q}{2} \times (f_{S,\theta} + f_{S,\theta}^3 \times f_{S,2\theta}) + q \times (1 + f_{S,\theta}^2 \times f_{S,2\theta}) + p \times f_{S,\theta} \times f_{S,2\theta} \right) \\
4) \quad & T_1 \times \left(\frac{1-p-2 \times q}{2} \times (f_{S,\theta}^2 \times f_{S,2\theta} + f_{S,\theta}^2 \times f_{S,2\theta} \times f_{S,4\theta}) + q \times (f_{S,\theta} + f_{S,\theta} \times f_{S,2\theta}) + p \right) \\
5) \quad & T_1 \times \left(\frac{1-p-2 \times q}{2} \times (f_{S,\theta}^2 + f_{S,\theta}^3 \times f_{S,3\theta}) + q \times (f_{S,\theta} + f_{S,\theta}^2 \times f_{S,3\theta}) + p \right)
\end{aligned}$$

2. Model Results

We turn to analyze the six dipping patterns. We start with an example plot, for $S = 10$ and $\theta = 45^\circ$, in Figure 35.

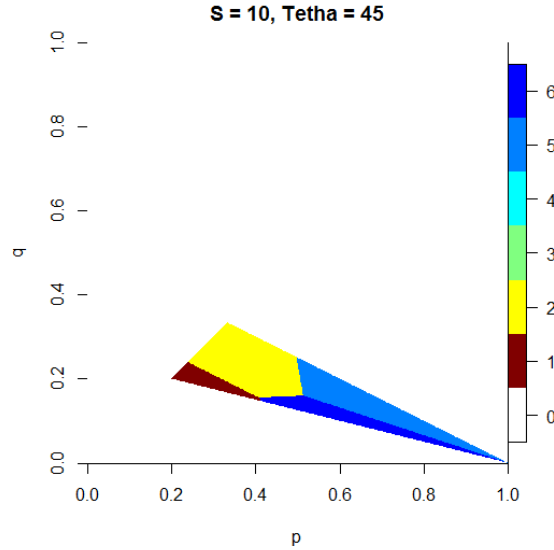


Figure 35. Five Rays Model $S = 10$, $\theta = 45^\circ$

The white part in the plot, like in the three rays model, corresponds to values of p and q that do not satisfy our assumptions ($p + 2 \times q \leq 1$ and $p > q > \frac{1-p-2 \times q}{2}$). We see that only four out of the six patterns actually show up. Patterns 3 and 4, which

involve significant jumping over rays are never optimal. We also see that for large values of p , patterns 5 and 6 are dominant, which is what we would expect since they are the patterns that dip in the central ray first. For large values of q , patterns 2 and 5 are dominant, which is also expected since these are the patterns that leave the rr and ll rays to be dipped last.

We now examine how a change in S and θ affects our results. We start by holding S constant at $S = 10$ and varying θ . The results appear in Figure 36.

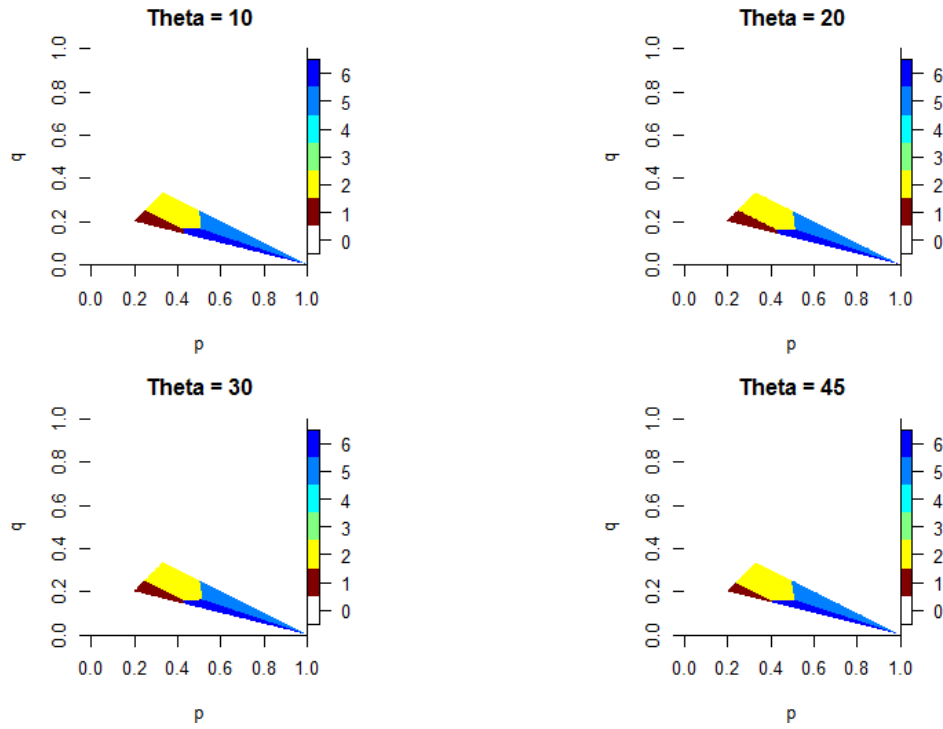


Figure 36. Five Rays Model, Ratio =10, Varying Angle

We barely see any difference between the plots. That is, when the helicopter is ten times faster than the submarine, which is a realistic assumption, the angle between rays, θ , does not affect our dipping order.

Our next step is to see how changing the speed ratio affects the pattern chosen. We choose $\theta = 30$ and vary the speed ratio. The results appear in Figure 37.

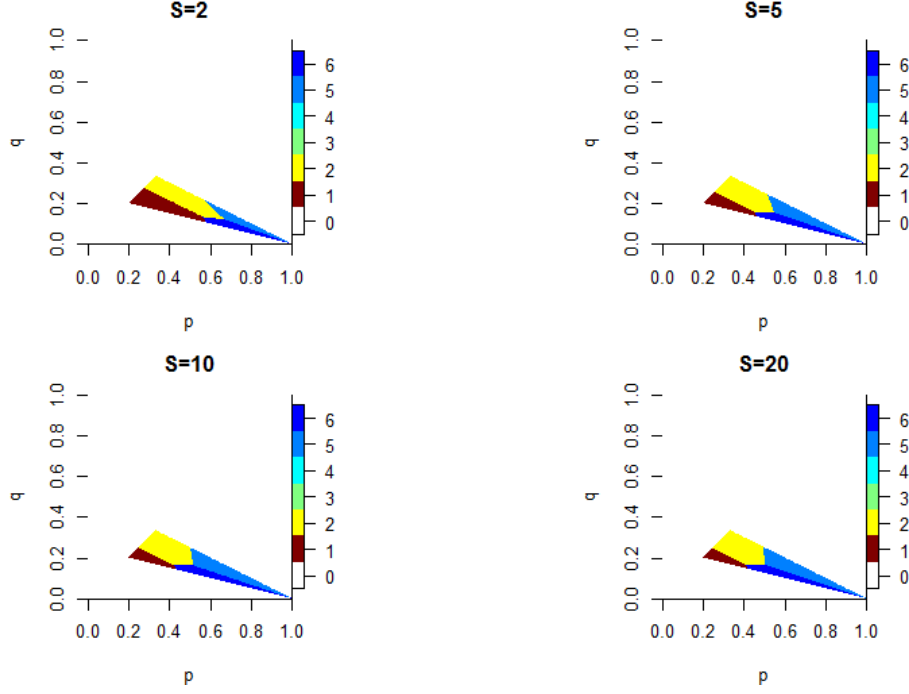


Figure 37. Five Rays Model, $\theta = 30$, S Varied

What we see in Figure 37 is that the faster the helicopter flies, the more likely we are to choose pattern 5 and 6 over 1 and 2. That is, we are more likely to start in the middle and jump over rays. This effect is similar to the one that happened when we looked at the angle. The faster the helicopter is, or the smaller the angle, the less “penalty” we get for jumping over them, and thus we are more likely to do so.

We note that if we expand the rays model into an infinite number of rays, we would expect to get the same results we saw in Chapter II and the continuous model.

C. THREE WEDGES MODEL

Our next model combines the ideas developed in Chapter II and the earlier sections of Chapter III. Instead of looking at rays, we now look at wedges.

1. Model Description

The submarine can travel along any ray from the datum inside a wedge, but different wedges may have different probabilities for the submarine presence. We denote

the angular size of the wedges by α, β and γ , and assign to these wedges the probabilities p, q and $1 - p - q$ respectively, as shown in Figure 38.

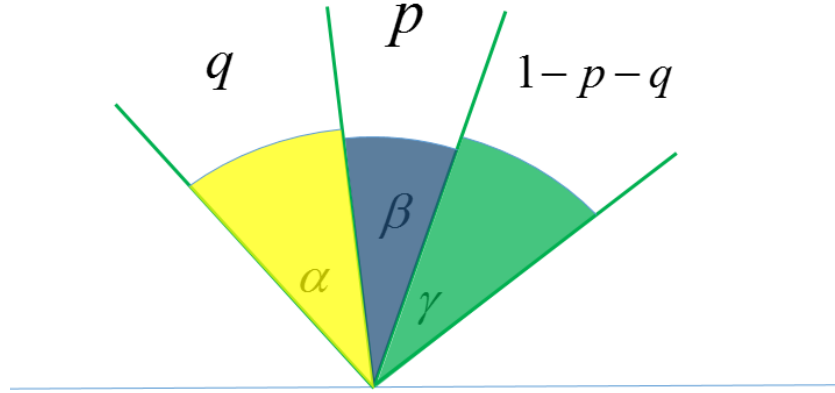


Figure 38. Three Wedges Model

We assume that the conditional probability distribution of the trajectory of the submarine along a ray from the datum within each wedge is uniform, and therefore the dipping pattern developed in Chapter II will also be optimal within the wedge, with one difference—the helicopter does not have to cover a 360-degree angle. Since the model developed is optimal for any dip along the way, it is also optimal if the helicopter does not need to cover the entire 360 degrees and the only change needed is the “when to stop” condition. We use this model to compute the expected time to detection. The next question is in what order do we dip the wedges. Like with the rays models, we would like to avoid “jumping” over wedges, but we expect that given certain conditions this may happen. The possible dipping orders are the same as in the three rays model, which are (l-left, c-center, r-right):

1. $l \rightarrow c \rightarrow r$
2. $l \rightarrow r \rightarrow c$
3. $c \rightarrow l \rightarrow r$

4. $c \rightarrow r \rightarrow l$
5. $r \rightarrow l \rightarrow c$
6. $r \rightarrow c \rightarrow l$

This model has more inputs than the rays models since we consider a different angle for each wedge.

2. Model Results

As in the model in Section B, we start with a basic scenario where $\alpha = \beta = \gamma = 30^\circ$ and $S = 10$. The results appear in Figure 39.

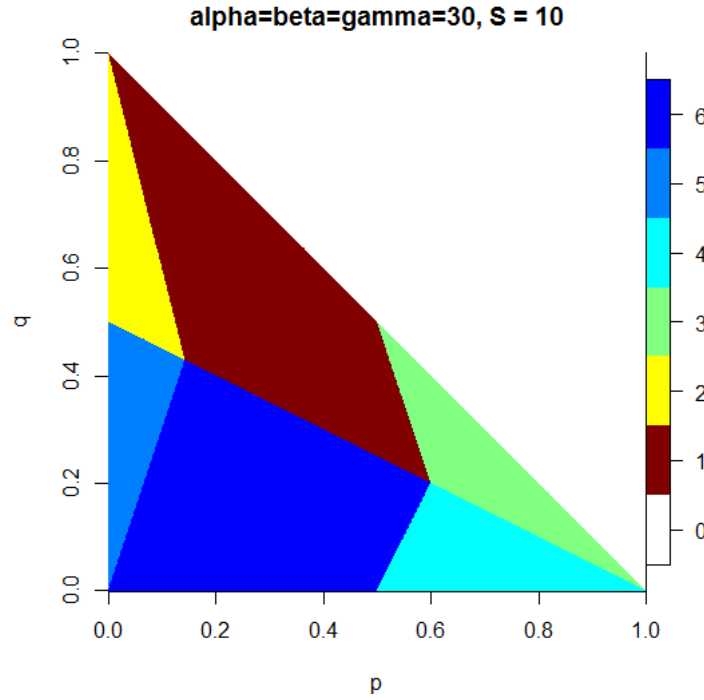


Figure 39. Three Wedges Model, $\alpha = \beta = \gamma = 30^\circ$, $S = 10$

We see that the larger p is (probability of the target in the central wedge), the more likely we are to start in the middle (patterns 3 and 4). The larger that q is (probability of the target in the left wedge), the more likely we are to start at the left (patterns 1 and 2).

We now examine the effect of the α and γ on the optimal dipping pattern. We vary them together, keeping all other parameters constant ($\beta = 30^\circ, S = 10$). The results appear in Figure 40.

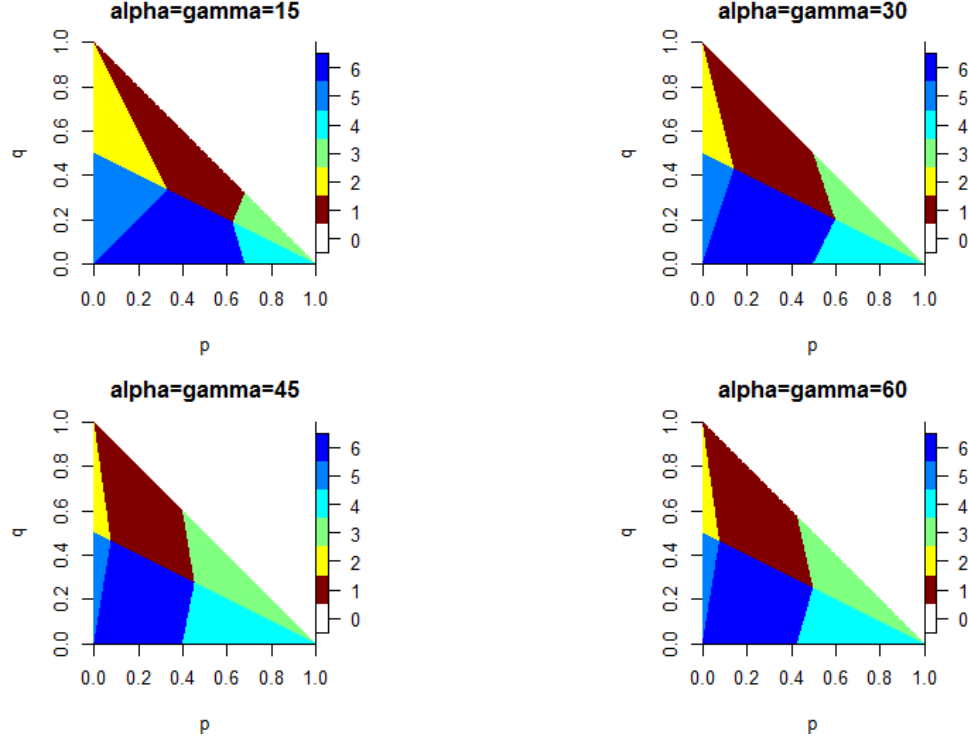


Figure 40. Three Wedges Model, $S = 10, \beta = 30^\circ, \alpha$ and γ Varied

We see that increasing the angles of the side wedges decreases the effectiveness of patterns 2 and 5. This means that in such situations it is less effective to start in a side wedge, move to the other side wedge and finish in the center. The reason this happens is that if we dip in one side wedge and then the other, we have to fly back to the center, over the wedge we already covered, and that becomes more expensive the wider the wedge is. We can also see that patterns 3 and 4 become more effective the wider the side wedges are. This happens since the wider the side wedges are, the less “dense” they are in terms of probability per unit angle (the probability of the wedge is constant, so the wider the wedge, the smaller the probability per unit angle). Since the side wedges are less dense, the central one becomes more attractive.

We now keep $\alpha = \gamma = 30^\circ$ and examine what happens when we vary β . The results appear in Figure 41.

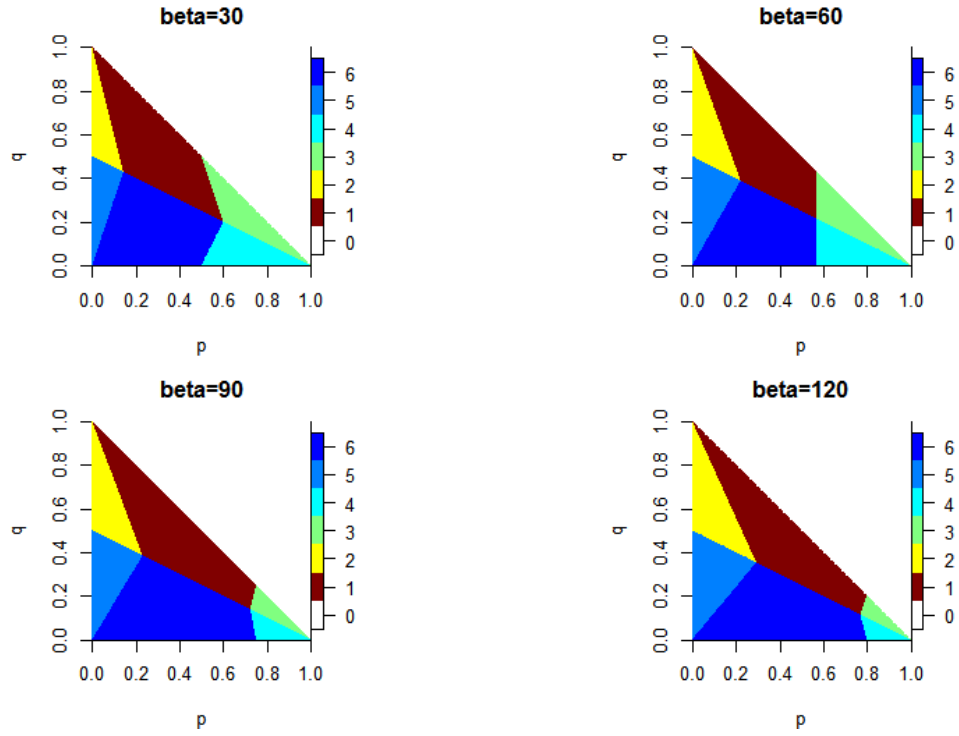


Figure 41. Three Wedges Model, $S = 10, \alpha = \gamma = 30^\circ$ and β Varied

We see here the opposite effect to the one we saw when varying the side wedges. When the central wedge grows, the less “dense” it is, and we are more likely to keep it for last (patterns 2 and 5) and less likely to start with it (patterns 3 and 4).

So far, we have examined symmetrical scenarios only ($\alpha = \gamma$). We now examine the scenario where $\alpha = \beta = 30^\circ$, and we vary γ . The results appear in Figure 42.

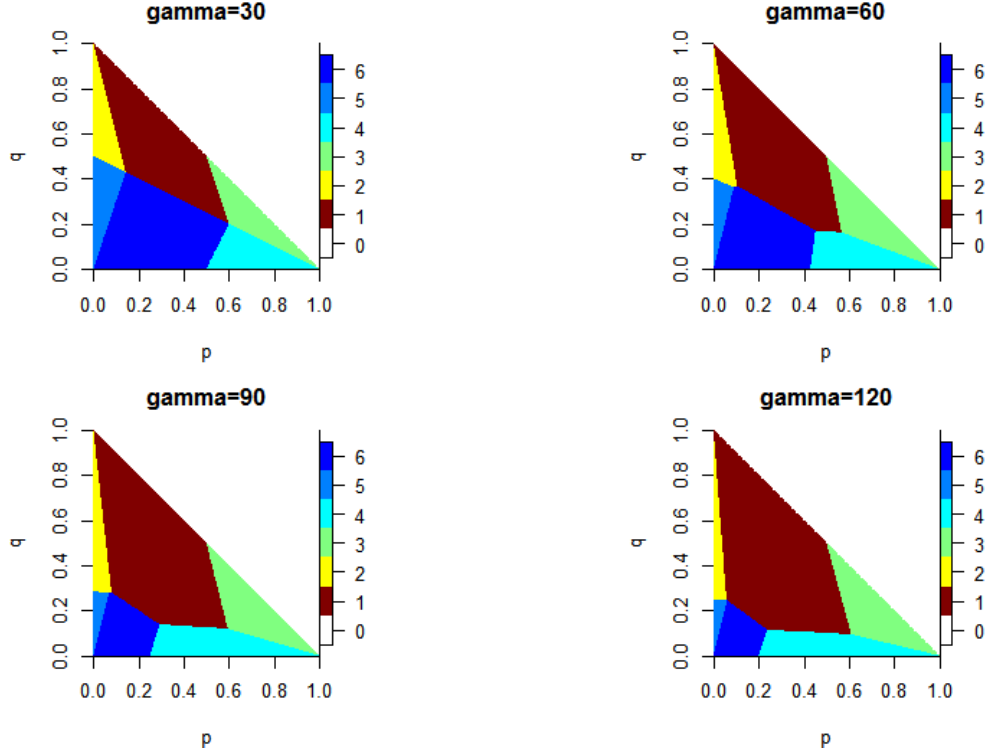


Figure 42. Three Wedges Model, $S = 10, \alpha = \beta = 30^\circ$ and γ Varied

The first thing we notice is that the results are no longer symmetrical. In Figures 40 through 43, patterns 4, 5, and 6 were mirroring patterns 1, 2, and 3. This happens because if $\alpha = \gamma$ we can switch q with $1 - p - q$, and we get a mirrored version of the problem; left becomes right but the rest stays the same. We also notice that the main effect of increasing γ is increasing the effectiveness of pattern 1 ($l \rightarrow c \rightarrow r$, colored red) compared to patterns 5 and 6. The other pattern that becomes more effective is pattern 3 ($c \rightarrow l \rightarrow r$, colored light green), compared to pattern 4. These are the two patterns that visit the right side wedge last. As before, when the wedge grows, it becomes less attractive and more likely to be visited last.

The last parameter we vary is the speed ratio between the helicopter and the submarine. We use $\alpha = \beta = \gamma = 30^\circ$ and vary the speed ratio to get the results that appear in Figure 43.

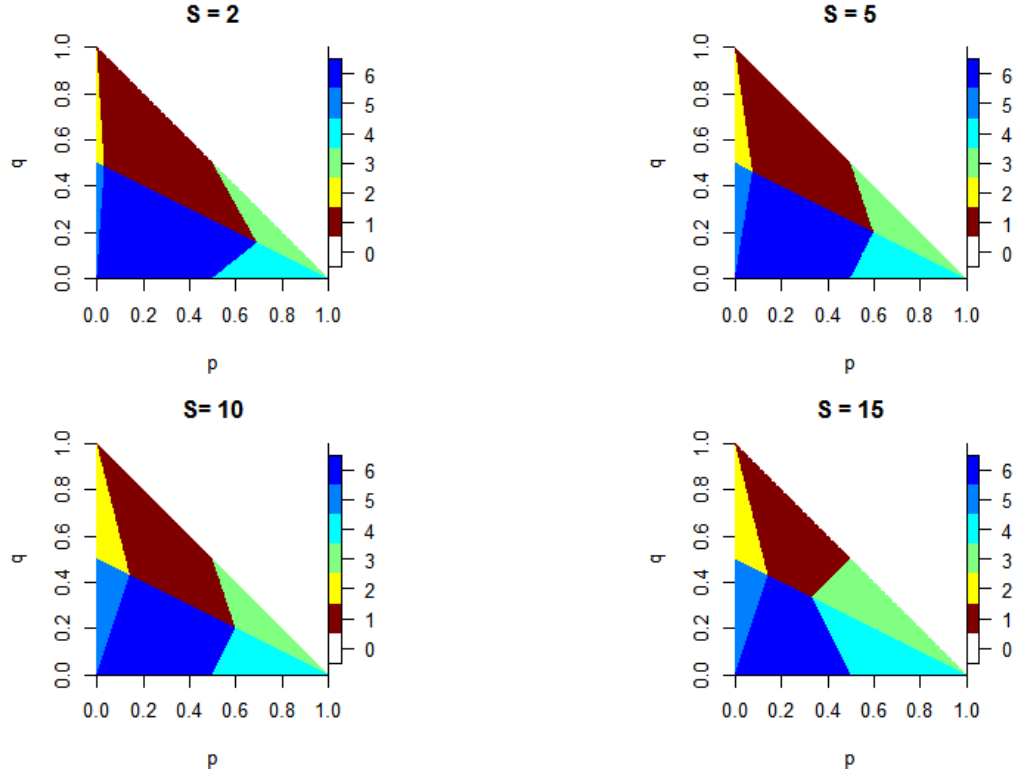


Figure 43. Three Wedges Model, $\alpha = \beta = \gamma = 30^\circ$, S Varied

Looking at the results, it is clear that when the speed ratio increases, patterns 1 and 6 become less effective and patterns 2, 3, 4, and 5 become more effective. Patterns 1 and 6 are the patterns that do not involve “jumping” over wedges (i.e., patterns $l \rightarrow c \rightarrow r$ and $r \rightarrow c \rightarrow l$). The faster the helicopter flies, the less “penalty” it gets for jumping over wedges. These results are consistent with results we got in other models.

IV. PAYLOAD OPTIMIZATION

In this chapter, we address a different problem. Since helicopters are very limited in the weight and volume they can carry, the payload the helicopter carries has a significant impact on mission effectiveness. The helicopter's payload includes fuel ("lungs"), sensors ("eyes"), and, in case of an attack mission, torpedoes ("fists"). In this chapter, we examine the optimal payload according to mission profile. To simplify the problem, we address only buoys and not a dipper in this chapter. As explained in Chapter II, Section F, we can use the same model developed in Chapter II to estimate probability of detection of buoys. Note that since this work is unclassified, the helicopter and system data are taken from open sources (the Sikorsky, Forecast International's Aerospace Portal, Wikipedia, and FAA websites).

The data used for this chapter's analysis include:

- Fuel efficiency: $100 * ((V^2 / 4000 - 3 * V / 28 + 13)$ lbs./hr., approximation based on Naval Air Systems Command (2000), where V is the helicopter's speed
- Fuel capacity—590 gallons (Forecast International 2016)
- Fuel weight—6 lbs./Gallon (FAA 2016)
- Helicopter's empty weight—13,470 lbs., (Sikorsky 2016)
- Helicopter's maximum takeoff weight—22,420 lbs. (Sikorsky 2016)
- Buoy detection radius—1 NM, estimate
- Buoy weight—15 lbs., estimate
- Torpedo weight—800 lbs (Wikipedia 2016)
- Time to launch buoys—immediate, estimate

A. DETECTION MISSION

On detection missions, the helicopter clearly does not need to carry torpedoes and only needs to balance its sensors and fuel. We can use our model from Chapter II to calculate the probability of detection given the limitations on fuel and the number of sensors. In all scenarios in this chapter, we assume the helicopter behaves optimally given the scenario parameters. For example, if we look at the case where the arrival time is 1 hour, and we carry 20 buoys, we are left with 230 gallons of fuel, which is enough to drop 17 out of the 20 buoys, and translates into ~ 0.3 probability of detection. Figure 44 illustrates the effect of changing the number of buoys carried. In this scenario, we assume a 1-hour arrival time to the datum, $V = 100, U = 8$.

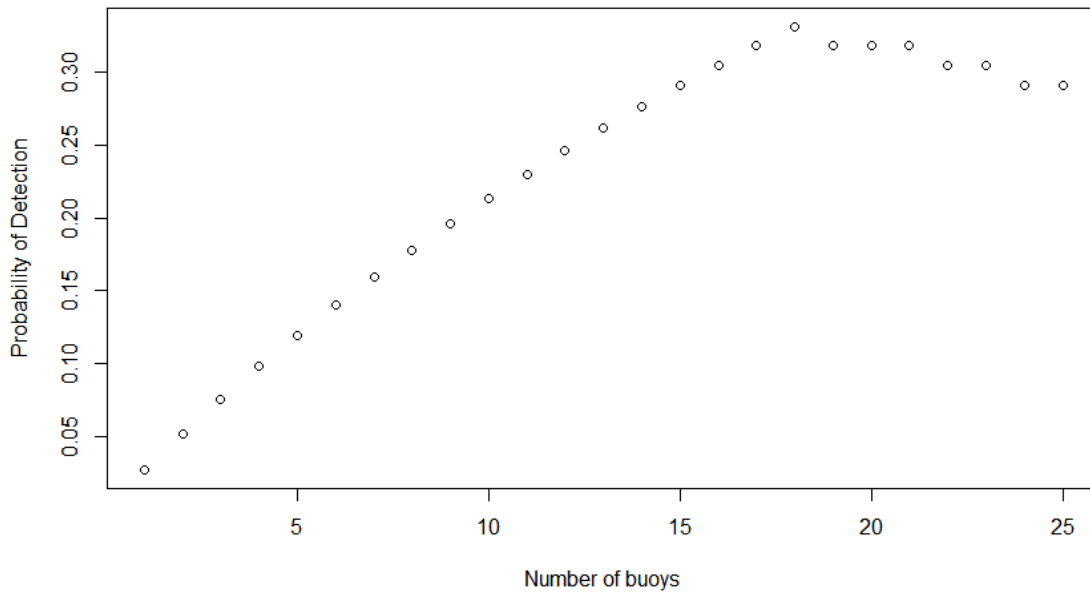


Figure 44. Probability of Detection vs. Number of Buoys, Arrival Time 1 Hour, Speed Ratio 10

From Figure 44, we see that the optimal payload of sonobuoys is 18 buoys, which results in a probability of detection of 0.33. The rest of the weight is used to carry fuel. If the helicopter carries fewer buoys than that, it will run out of buoys while still having

enough endurance to deploy more buoys. If the helicopter carries more buoys, it will run out of fuel while it still has buoys available for deployment.

We now examine how the arrival time affects the number of buoys the helicopter should carry. To do so, we go through the same analysis we did before but this time for several arrival times, $V = 100, U = 8$. The results appear in Figure 45.

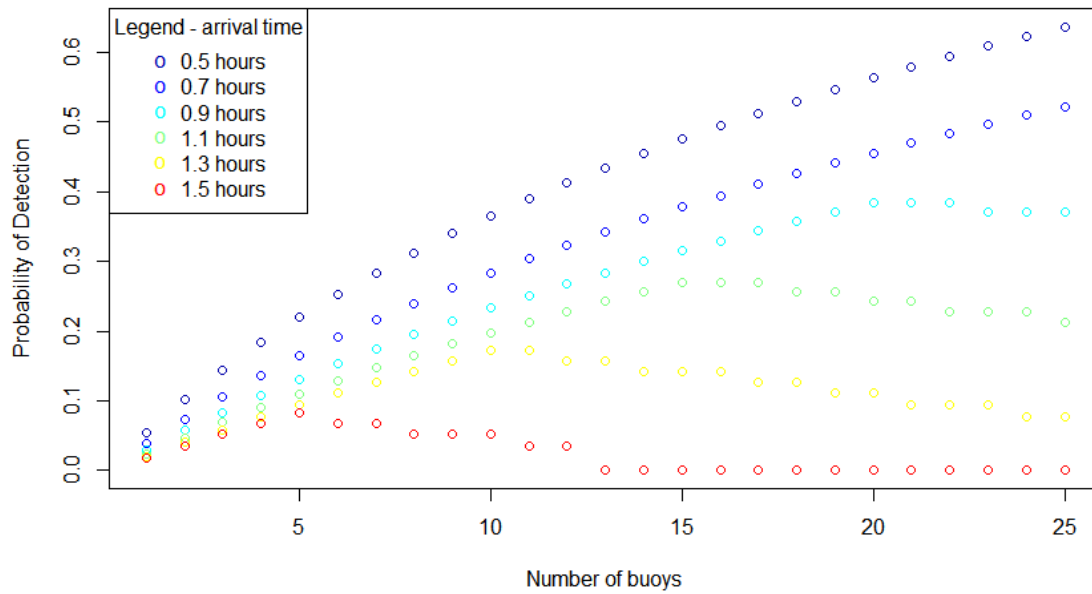


Figure 45. Coverage vs. Number of Buoys, Arrival Time Varied

As we saw earlier, the later we arrive, the less likely we are to find the submarine. We can also see that the later we arrive, the fewer buoys we should take. This is because we need more fuel in order to travel back and forth from the AoU, and so we cannot afford as many buoys as we could when we arrive sooner. We also see that we cannot arrive to the AoU much past an hour and a half late, because we will not be able to take any buoys.

B. ATTACK MISSION

We now continue our analysis with attack missions. In an attack mission, the helicopter also needs to carry torpedoes. Carrying too many sensors with not enough torpedoes will result in a detection but no kill (which we consider a mission fail). Carrying too many torpedoes will result in fewer sonobuoys, which will result in reduced detection capability. We also add the torpedoes' probability of kill to the list of parameters.

The probability of mission success is now the probability the helicopter detects the submarine, times the probability the helicopter hits the submarine given it detects the sub. In math form $P_{suc} = P_{det} \times (1 - (1 - P_k)^n) = P_{det} \times (1 - e^{-n \times \log(1/P_k)})$ where P_k is the probability of kill for one torpedo and n is the number of torpedoes carried by the helicopter. We assume the results of the torpedoes are independent.

We now calculate, for each combination of buoys and torpedoes, the probability of detection using Section A of this chapter and the probability of mission success. Single mission results (in this case for arrival time of 35 minutes and $P_k = 0.7, V = 100, U = 8$) appear in Figure 46.

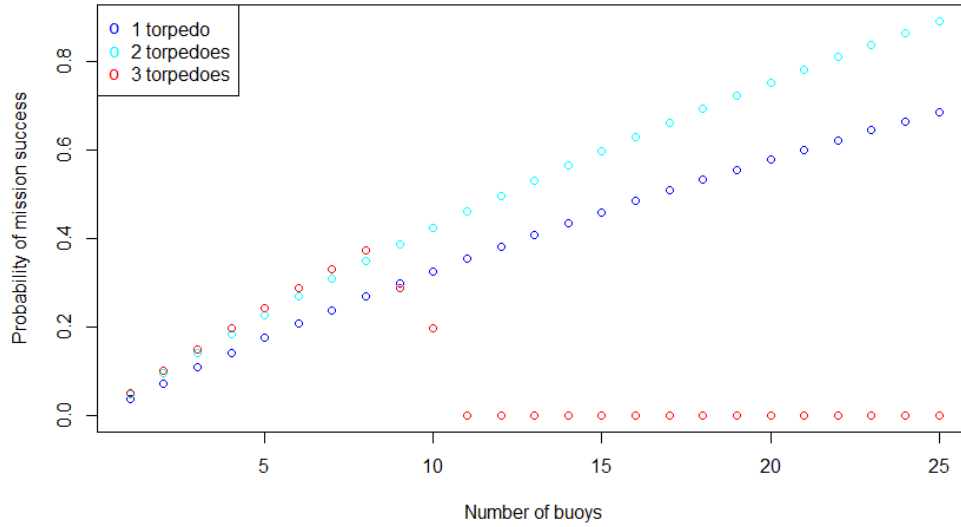


Figure 46. Probability of Mission Success with Different Number of Torpedoes

Figure 46 presents the probability of mission success for different mixes of torpedoes and buoys. In this case, we see that the optimal payload is two torpedoes and 25 buoys, which ensures a probability of success of approximately 0.9. We also see that for three torpedoes we cannot afford to carry more than ten buoys.

We now analyze the effect of the arrival time and torpedoes' probability of kill on the optimal payload and the probability of mission success. We start with arrival time. For a given number of torpedoes (1, 2, 3) and arrival time, we plot the probability of mission success where the number of buoys is determined optimally. The results appear in Figure 47.

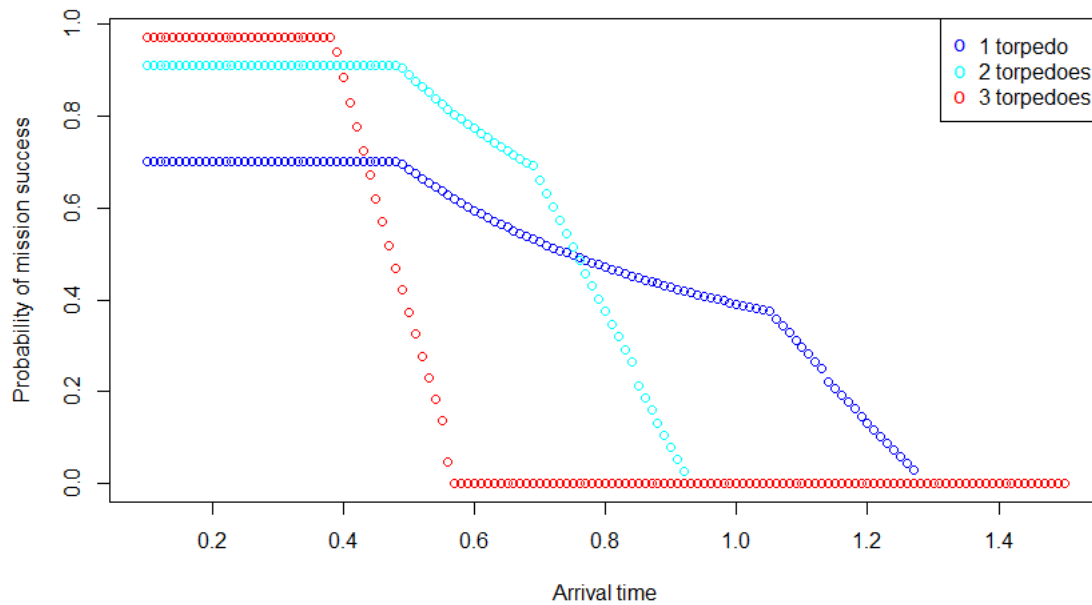


Figure 47. Probability of Success vs. Arrival Time

The first thing we notice is the interesting shape of the plots. We focus on the dark blue line of 1 torpedo. For a fast arrival time, detection is guaranteed, and therefore the probability of mission success is the probability of kill by a single torpedo. If the helicopter arrives later than half an hour, we cannot assure detection, and therefore, the probability of success starts to decline. If we arrive more than an hour later (around 1.1 hours, to be precise), the helicopter can no longer carry 25 buoys, and therefore, the

probability of detection (and with it the probability of mission success) starts to drop significantly up to a point where the helicopter cannot carry enough fuel to even get to the datum (around 1.3 hours). Figure 47 also gives us the optimal number of torpedoes for any arrival time (3 for $T_a < 0.4$, 2 for $0.4 < T_a < 0.8$ and 1 for $T_a > 0.8$).

We next examine the effect P_k has on the optimal payload and probability of mission success. In Figure 48 we see four graphs similar to Figure 47, but with different P_k .

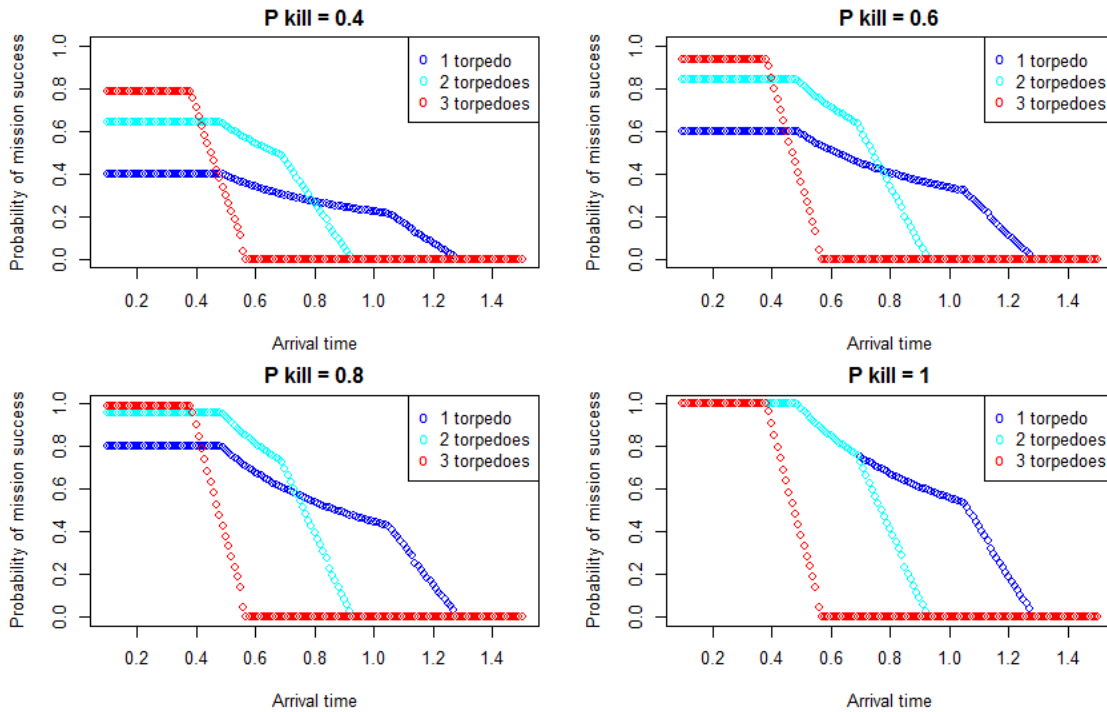


Figure 48. Probability of Success vs. Arrival Time, Varying P_k

As we expect, varying P_k affects the single torpedo case the most and the three torpedoes case the least. We can see that increasing P_k increases the probability of mission success, but it does not significantly change the optimal payload. The more effective the torpedoes are, the fewer of them we should carry, but this effect is not significant.

V. CONCLUSION

A. SUMMARY

In this thesis, we analyze ASW missions, focusing on MH-60R helicopters. The first scenario we study is a helicopter sent out to detect a submarine after an initial cue given by an external source, with no information regarding the submarine's bearing. We present a dipping pattern and prove its optimality in this scenario. We then analyze the effect of the scenario parameters: a) submarine speed, b) helicopter speed, c) time late, d) dipper detection radius, and e) time it takes to dip, on the time it would take the helicopter to detect the submarine. We show that time late is the most important parameter, and therefore, minimizing the time it takes to get the helicopter ready to fly is the best way to improve the probability of detecting the submarine. We also analyze the use of sonobuoys instead of a dipper and the differences between the two options, including the trade-off of a sensor's detection radius and the time it takes to use it. The last section of Chapter II briefly discusses a scenario where the submarine's speed is not known, and we have two possible speeds. We approach the problem as two consecutive single-speed scenarios and show how to execute such a plan.

We then analyze a scenario in which we do have some information regarding the submarine's bearing. We create three models to analyze this scenario: a) three rays model, b) five rays model, and c) three wedges model. We analyze the effect the quality of information—how well the helicopter knows the submarine's bearing, and speeds of the submarine and helicopter—has on the optimal behavior (dipping order) of the helicopter.

We then analyze the payload of an MH-60R helicopter in an ASW mission. Since the helicopter can carry fuel, sensor, and torpedoes, but is limited by the weight and volume it can carry, the payload decision has a significant effect on the probability of mission success. We analyze two types of missions: a) detection missions and b) attack missions. In the detection mission analysis, we present the trade-off between fuel and sensors (sonobuoys) and show how different scenarios require different payloads in order

to maximize the probability of detection. In the attack mission analysis, we show the trade-off between probability of detection (fuel and sensors) and probability of kill (torpedoes). We give examples of scenarios in which more fuel and sensors (optimized in the way offered in the detection mission analysis) are recommended, and scenarios in which more torpedoes will result in a better probability of mission success. In both types of missions, we show that the optimal payload varies significantly according to the mission parameters, mainly the time it takes the helicopter to fly to the AoU.

B. FOLLOW-ON WORK

The models presented in this thesis are based on a set of assumptions. Relaxing any of these assumptions will change the optimality of our model and new models can be developed and analyzed. We propose future work should relax the following assumptions:

- The submarine's speed is known—In Chapter II, Section E, we examine a two speeds model. Expanding this idea to a different distribution of the submarine's speed may result in different optimal dipping patterns.
- Perfect initial detection—uncertainty in the position of the initial detection, which was not discussed in this thesis, will expand the AoU and change its shape.
- Cookie cutter sensors—throughout this thesis we assume that if the helicopter dips and the target submarine is within detection range, the submarine is detected. This is, of course, not the case in real operational scenarios. This means that when the helicopter dips we can no longer be sure there is no target in the dipped area, but the probability of a target being present in it is reduced.

In this thesis, we did not combine sonobuoys with a dipper. An analysis of both the search pattern and the optimal payload in such a scenario might offer operational benefits.

Another aspect not discussed in this work is the cooperation of two or more helicopters in one mission. The benefits of this approach are not straightforward and simply dividing the problem into two might not be the optimal way to go.

LIST OF REFERENCES

- FAA, Weight and balance, *Helicopter Flying Manual*. Accessed August 02, 2016, www.faa.gov/regulations_policies/handbooks_manuals/aviation/helicopter_flying_handbook/media/hfh_ch06.pdf
- Forecast International Aerospace Portal. MH-60R- Seahawk. Accessed August 02, 2016, <http://www.bga-aeroweb.com/Defense/MH-60R-Seahawk.html>
- Forrest RN (1993) *Estimating Search Effectiveness with Limited Information* (Naval Postgraduate School, Monterey, CA).
- Haley BK, Stone LD (1980) *Search Theory and Applications* (Plenum Press, New York)
- Koopman BO (1946), *Search and Screening*, 1st edition (operations evaluation group, office of the chief of naval operations, navy department, Washington, DC).
- Kuhn T (2014) Optimal sensor placement in active multistatic sonar networks. Master's thesis, Naval Postgraduate School, Monterey, CA.
- Naval Air Systems Command (2000) *NATOPS Flight Manual Navy Model SH-60B Aircraft* (NAVAIR, Patuxent River, MD)
- Shephard RW, Hartley DA, Haysman PJ, Thorpe L and Bathe MR (1988) *Applied Operations Research* (Plenum Publishing Corporation, New York).
- Sikorsky . MH-60R. Accessed August 02, 2016, <http://www.mh-60.com/mh-60r/>
- Stone LD (1975) *Theory of Optimal Search* (Academic Press, New York)
- Stone LD, Royset J, Washburn A (2016), *Optimal Search of Moving Targets* (Springer International Publishing, Switzerland)
- Washburn A (1978) *Search for a Moving Target: Upper Bound on Detection Probability*, (Naval Postgraduate School, Monterey, CA).
- Washburn A (1980) *Expanding Area Search Experiments* (Naval Postgraduate School, Monterey, CA).
- Washburn A (2002) *Search and Detection*, 4th edition (Institute for Operations Research and the Management Sciences, Linthicum, MD).
- Wikipedia, mark 50 torpedo, Accessed August 02, 2016, http://en.wikipedia.org/wiki/Mark_50_torpedo

THIS PAGE INTENTIONALLY LEFT BLANK

INITIAL DISTRIBUTION LIST

1. Defense Technical Information Center
Ft. Belvoir, Virginia
2. Dudley Knox Library
Naval Postgraduate School
Monterey, California